

CAPITAL UNIVERSITY OF SCIENCE AND
TECHNOLOGY, ISLAMABAD



**Darcy-Forchheimer Casson
Nanofluid Flow between
Horizontal Plates**

by

Haseeb Ur Rahman

A thesis submitted in partial fulfillment for the
degree of Master of Philosophy

in the

Faculty of Computing

Department of Mathematics

2022

Copyright © 2022 by Haseeb Ur Rahman

All rights reserved. No part of this thesis may be reproduced, distributed, or transmitted in any form or by any means, including photocopying, recording, or other electronic or mechanical methods, by any information storage and retrieval system without the prior written permission of the author.

*I dedicate my dissertation work to my **family** and dignified **teachers**. A special feeling of gratitude to my loving parents who have supported me in my studies.*



CERTIFICATE OF APPROVAL

Darcy-Forchheimer Casson Nanofluid Flow between Horizontal Plates

by

Haseeb Ur Rahman

(MMT191026)

THESIS EXAMINING COMMITTEE

| S. No. | Examiner | Name | Organization |
|--------|-------------------|---------------------------|---------------------------|
| (a) | External Examiner | Dr. Nabeela Kousar | AIR University, Islamabad |
| (b) | Internal Examiner | Dr. Rashid Ali | CUST, Islamabad |
| (c) | Supervisor | Dr. Dur-e-Shehwar Sagheer | CUST, Islamabad |

Dr. Dur-e-Shehwar Sagheer
Thesis Supervisor
November, 2022

Dr. Muhammad Sagheer
Head
Dept. of Mathematics
November, 2022

Dr. M. Abdul Qadir
Dean
Faculty of Computing
November, 2022

Author's Declaration

I, **Haseeb ur Rahman** here by state that my MPhil thesis titled “**Darcy-Forchheimer Casson Nanofluid Flow between Horizontal Plates**” is my own work and has not been submitted previously by me for taking any degree from Capital University of Science and Technology, Islamabad or anywhere else in the country/abroad.

At any time if my statement is found to be incorrect even after my graduation, the University has the right to withdraw my MPhil Degree.

(Haseeb ur Rahman)

Registration No: MMT191026

Plagiarism Undertaking

I solemnly declare that research work presented in this thesis titled “**Darcy-Forchheimer Casson Nanofluid Flow between Horizontal Plates**” is solely my research work with no significant contribution from any other person. Small contribution/help wherever taken has been duly acknowledged and that complete thesis has been written by me.

I understand the zero tolerance policy of the HEC and Capital University of Science and Technology towards plagiarism. Therefore, I as an author of the above titled thesis declare that no portion of my thesis has been plagiarized and any material used as reference is properly referred/cited.

I undertake that if I am found guilty of any formal plagiarism in the above titled thesis even after award of MPhil, the University reserves the right to withdraw/revoke my MPhil and that HEC and the University have the right to publish my name on the HEC/University website on which names of students are placed who submitted plagiarized work.

(Haseeb ur Rahman)

Registration No: MMT191026

Acknowledgement

Starting with the name of Almighty **ALLAH** who is most gracious and omnipresent, who makes the mankind and created this world to reveal what is veiled. Also, the **Prophet Muhammad (Peace Be Upon Him)** who is a guidance in every aspect of life for the betterment of Humanity. Firstly, I would like to express my deepest appreciation to my supervisor **Dr. Dur-e-Shehwar Sagheer**, for the continual support of my MPhil research and also for her immense knowledge and enthusiasm. Without her tireless help, I would have not been able to commence this present research work. I could not have imagined having a better mentor and supervisor for my MPhil thesis. Besides my supervisor, I owe my profound gratitude to **Dr. Muhammad Sagheer** for his superb guidance and inexhaustible inspiration throughout this thesis. Without his tireless help, I would have not been able to commence this current research study. I am truly thankful to my teachers at Capital University of Science and Technology, **Dr. Rashid Ali, Dr. Abdul Rehman Kashif, Dr. Muhammad Afzal, Dr. Samina Rashid** and **Dr. Shafqat Hussain**. They are excellent teachers and I learnt a lot from them throughout the course of my MPhil study. My most sincere and warm wishes to my friends especially university fellows **Raja Bilal Javed, Sajid Ali Satti, Raja Qasim Mehmood, Zafran Sajid, Abdul Rehman** and **Faisal Mehmood** who were always there as a source of encouragement for me. Further on, I am grateful to my colleagues **Dr. Qasim Mehmood, Shahzad Munir Ansari, Adil Ahmed**, my parents, wife and sibling for supporting me spirituality all over my life.

(Haseeb ur Rahman)

Abstract

This research is mainly concerned with the characteristics of magnetohydrodynamics and Darcy-Forchheimer medium in nanofluid flow between two horizontal plates. A uniformly induced magnetic impact is involved in the direction normal to the lower plate. Darcy-Forchheimer medium is considered between the plates that allow the flow along horizontal axis with additional effects of porosity and friction. The features of Brownian diffusive motion and thermophoresis are disclosed. Governing equations are transformed into a non-linear boundary value problem, which is numerically solved by shooting method. This numerical technique is incorporated using Runge-Kutta method of order four and Newton method. Graphs are plotted to depict different significant effects.

Contents

| | |
|---|-------------|
| Author's Declaration | iv |
| Plagiarism Undertaking | v |
| Acknowledgement | vi |
| Abstract | vii |
| List of Figures | x |
| Abbreviations | xii |
| Symbols | xiii |
| 1 Introduction | 1 |
| 1.1 Thesis Contribution | 3 |
| 1.2 Thesis Outline | 4 |
| 2 Basic Definitions and Governing Equations | 5 |
| 2.1 Properties of fluids | 5 |
| 2.2 Types of Fluid | 7 |
| 2.3 Types of Fluid Flow | 9 |
| 2.4 Modes of Heat Transfer | 11 |
| 2.5 Dimensionless Numbers | 12 |
| 2.6 Governing Laws | 14 |
| 2.7 Shooting Method | 15 |
| 3 Darcy-Forchheimer Nanofluid Flow between Horizontal Plates | 18 |
| 3.1 Introduction | 18 |
| 3.2 Mathematical Modeling | 19 |
| 3.3 Numerical Treatment | 27 |
| 3.4 Results and Discussions | 32 |
| 4 MHD Squeezed Darcy-Forchheimer Casson Fluid Flow between Horizontal Plates | 43 |

| | | |
|----------|------------------------------------|-----------|
| 4.1 | Introduction | 43 |
| 4.2 | Mathematical Modeling | 44 |
| 4.3 | Numerical Treatment | 48 |
| 4.4 | Representation of Graphs | 54 |
| 5 | Conclusion | 66 |
| | Bibliography | 68 |

List of Figures

| | | |
|------|--|----|
| 3.1 | Geometry of the problem. | 19 |
| 3.2 | Consequences of Fr on $f(\eta)$ | 34 |
| 3.3 | Consequences of Fr on $f'(\eta)$ | 34 |
| 3.4 | Consequences of M on $f(\eta)$ | 35 |
| 3.5 | Consequences of M on $f'(\eta)$ | 35 |
| 3.6 | Consequences of P on $f(\eta)$ | 36 |
| 3.7 | Consequences of P on $f'(\eta)$ | 36 |
| 3.8 | Consequences of P on $\theta(\eta)$ | 37 |
| 3.9 | Consequences of Nb on $\theta(\eta)$ | 37 |
| 3.10 | Consequences of Nt on $\theta(\eta)$ | 38 |
| 3.11 | Consequences of P on $\phi(\eta)$ | 38 |
| 3.12 | Consequences of Nb on $\phi(\eta)$ | 39 |
| 3.13 | Consequences of Nt on $\phi(\eta)$ | 39 |
| 3.14 | Variation in N_u for Viscosity Parameter P and Thermophoresis N_t | 40 |
| 3.15 | Variation in N_u for Viscosity Parametere P and Brownian Diffusion N_b | 40 |
| 3.16 | Variation in C_f for porosity factor λ | 41 |
| 3.17 | Variation in C_f for magnetic parameter M. | 41 |
| 3.18 | Consequences of P_r on $\theta(\eta)$ | 42 |
| 4.1 | Geometry of the problem. | 44 |
| 4.2 | Consequences of F_r on $f(\eta)$ | 56 |
| 4.3 | Consequences of F_r on $f'(\eta)$ | 56 |
| 4.4 | Consequences of M on $f(\eta)$ | 57 |
| 4.5 | Consequences of M on $f'(\eta)$ | 57 |
| 4.6 | Consequences of P on $f(\eta)$ | 58 |
| 4.7 | Consequences of P on $f'(\eta)$ | 58 |
| 4.8 | Consequences of P on $\theta(\eta)$ | 59 |
| 4.9 | Consequences of Nb on $\theta(\eta)$ | 59 |
| 4.10 | Consequences of Nt on $\theta(\eta)$ | 60 |
| 4.11 | Consequences of P on $\phi(\eta)$ | 60 |
| 4.12 | Consequences of Nb on $\phi(\eta)$ | 61 |
| 4.13 | Consequences of Nt on $\phi(\eta)$ | 61 |
| 4.14 | Nusselt number w.r.t P and N_t | 62 |
| 4.15 | Nusselt number w.r.t P and N_b | 62 |
| 4.16 | Variation in C_f for porosity factor λ | 63 |

| | | |
|------|---|----|
| 4.17 | Variation in C_f for magnetic parameter M . | 63 |
| 4.18 | Consequences of Pr on $\theta(\eta)$. | 64 |
| 4.19 | Skin friction w.r.t γ and λ . | 64 |
| 4.20 | Nusselt number w.r.t γ and λ . | 65 |

Abbreviations

| | |
|-------------|---------------------------------|
| IVPs | Initial value problems |
| MHD | Magnetohydrodynamics |
| ODEs | Ordinary differential equations |
| PDEs | Partial differential equations |
| RK | Runge-Kutta |

Symbols

| | |
|--------------|---|
| z | Stretching rate in s^{-1} |
| ρ | Density in kg m^{-3} |
| ν | Kinematic viscosity in m^2s^{-1} |
| k | Thermal conductivity |
| α | Thermal diffusivity in m^2s^{-1} |
| $u_1 = zx_1$ | Velocity in ms^{-1} |
| u_1 | Velocity component in ms^{-1} |
| u_2 | Velocity component in ms^{-1} |
| x_1 | Cartesian coordinates in m |
| x_2 | Cartesian coordinates in m |
| B_0 | Magnetic number |
| C_f | Skin friction |
| D_B | Brownian diffusion in m^2s^{-1} |
| D_T | Thermophoretic diffusion in m^2s^{-1} |
| M | Non dimensional magnetic number |
| MHD | Magnetohydrodynamics |
| Nb | Brownian diffusion parameter |
| Nt | Thermophoresis parameter |
| Nu | Nusselt number |
| P | Viscosity parameter |
| Pr | Prandtl number |
| $RK4$ | Runge-Kutta method |
| Sc | Schmidt number |

| | |
|------------|---|
| T | Temperature |
| ϕ | Nanoparticle volume fraction |
| R | Thermal radiation parameter |
| Ec | Eckert number |
| γ | Inclination Angle |
| σ_s | Electrical conductivity of the nanoparticle |
| f | Dimensionless velocity |
| θ | Dimensionless temperature |
| η | Independent similarity variable |
| h | Dimensionless concentration |
| C | Concentration |

Chapter 1

Introduction

Every physical scenario of viscous fluid in all material involves the natural phenomenon of heat and mass convection. In many different formations, including two parallel plates, extending surfaces, and inside a cylinder, this phenomenon occurs rather naturally. As a result, a fluid moving between two surfaces is referred to as squeezing flow. Researchers that study fluid flow, heat and mass transport have given significant attention to squeezing flow because of its importance and demand in industry. The fields of fluid dynamics that are specifically related to mechanical and biochemical engineering, food processing, chemical engineering, and industrial processing are typical examples of areas where the idea of squeezing flow is most frequently employed. Additionally, we have observed the example in automobile, lubricants, rolling elements, machine devices, and gears. The pioneer approach was reported by Rasool et al. [1] which is highly valued in scientific community with helpful remarks on the flow profiles, squeezing flow between two surfaces Rasool revealed for the first time in his research. Later, the squeezing flow was extensively covered in other articles. For example, Rashidi et al. [2] discussed unsteady and symmetric squeezed flow of nanofluids for approximation of analytic solutions to the flow problems 2015. In 2015, Hayat et al. [3] disclosed the features of three dimensional and squeezed flow using two parallel sheets because of mixed convection. Hayat et al. [4] reported squeezing flow in rotating frame between two disks. The problems were

developed using second grade fluid. In another study, Hayat et al. [5] discussed the findings of flow bounded by porous squeezed enclosure disclosing the features of magnetic field effects. Shahmohamadi and Rashidi [6] reported some good findings on the squeezing flow of nanofluids subject to rotating channel. The lower plate was assumed to be porous. Some recent studies [7],[8] are also referred for further understanding the above scenario. Nanofluids are a more effective formulation for fluid mechanics as a result of technological advancements. Typically, this formulation has metallic nanoparticles dispersed for a shorter time in the base fluid. The outcomes of this short term suspension, are quite powerful since they are more efficient and have more thermophysical characteristics, like density, thermal and electrical conductivity.

Nanofluids have made considerable strides due to the thermal properties and dynamic flexibility in the context of irreversibility, entropy and many other relevant qualities. The pioneer study was reported by Choi [9] illustrating the nanoparticle's effects on the underlying liquid's thermo-physical properties. The research community praised the idea favorably. Later, Parvin and Chamkha [10] reported free convection and entropy optimization of nanofluids flowing in odd shaped cavity. Zaraki et al. [11] disclosed the properties of boundary layer convection considering the size, type and shape of nanoparticles as well as the type of base fluid. Reddy and Chamkha [12] accounted the effect of Soret and Dufour on water and water type suspensions passing via stretching sheet. Chamkha et al. [13] disclosed the features of entropy optimization in water nanofluid using magnetic influence. Rasool et al. [14] discussed the effects of porosity and Darcy media in nanofluid flow via stretching surface. Ismael et al. [15] analyzed the entropy optimization in cavity filled with nanofluid via porous medium. Rasool et al. [16] reported flow of nanofluids bounded by a convective and vertically adjusted Riga plate. Many recent articles are typically based on the flow of nanofluids however, some of them are listed here [17–36].

Many essential mechanical and industrial processes use fluid flow analysis through porous media. Examples of typical methods that analyze fluid flow via porous material are the subsurface water purification process, oil recovery and purification,

outlining, pipe developments, and many more processes. Darcy's original definition of the earlier models called for weak porosity conditions and lower velocity. Later on, Forchheimer [37] remodeled it using nonlinear factor through velocity and the new name given to this model as Darcy-Forchheimer model. Muskat [38] presented homogeneous fluid flow through Darcy medium. Seddeek [39] disclosed the features of thermophoresis and dissipation in Darcy type fluid flow using the concept of mixed convection. Hayat et al. [40] used a bidirectional water based nanofluid flow subject to convective conditions to study the entropy optimization and heat and mass transmission mechanism. Sadiq and Hayat [41] reported nanofluid flow of the Darcy-Forchheimer type via a stretched surface that has been heated convectively. Umavathi et al. [42] reported numerical analysis of a rectangular duct with vertical adjustments enclosing a Darcy type nanofluid flow. Hayat et al. [43] conducted chemical reaction framework of radiation effect and heat generation in Darcy type nanofluid flow.

1.1 Thesis Contribution

In this research our motivation is based on three novel concepts. First, to involve two parallel plates with a gap filled with a porous medium that has been reported with limitations, include the magnetohydrodynamics (MHD) effect in this formulation, and finally, if examines the impact of the model's squeezing nature on the fluid flow analyse. The whole research is organised as follows. A viscous, MHD non-Newtonian nanofluid is investigated via Darcy medium between two parallel plates h apart. Brownian diffusive motion and thermophoresis are both involved. Second, applying appropriate transformations, the thus-formulated governing issues are turned into nonlinear dimensionless problems. Third, a numerical shooting technique is used in MATLAB to solve problems and collect data for the velocity field, temperature distribution, concentration distribution, and Nusselt number. All of the results have been graphed. Finally, a detailed discussion of the results is offered.

Fourth, the work of Rasool et al. [1] is extended by considering inclined magnetic field, Casson fluid, Viscous dissipation and chemical reaction over a permeable surface. To get the numerical results shooting technique endowed with Runge-Kutta method of order four and Newton method is used. Result and discussions are also provided with end of graphs.

1.2 Thesis Outline

This research work is further classified into four main chapters.

Chapter 2 covers some fundamental fluid definitions, terminologies, and governing equations that are required for the calculations of different variables like temperature, velocity, viscosity and magneticfield measurements.

Chapter 3 contains the review work of Rasool et al. [1]. The set of nonlinear PDEs into a set of nonlinear governing equations are converted ODEs by utilizing similarity transformation, which we then solve numerically. Through this research of the shooting technique, is used for numerical results for the set of nonlinear ODEs.

Chapter 4 extends the work of Rasool et al.[1] by considering squeezed hybrid nanofluid flow over a permeable sensor surface. The transformation of similarities has been utilized for the conversion of PDEs to ODEs. The transformed nonlinear ODEs are then solved by using the shooting technique that is most used for research work.

Chapter 5 summarizes the research work and gives the main conclusion arising from the whole study.

All the references used in this thesis are presented in Bibliography.

Chapter 2

Basic Definitions and Governing Equations

This chapter addresses some basic concepts, definitions and governing laws related to the fluid dynamics. Dimensionless quantities are also discussed which seem to be helpful in the subsequent chapters. Moreover, a brief discussion has been done for the numerical methodology adopted for the solution of governing equations.

2.1 Properties of fluids

This section contains, some basic terminologies and definitions from fluid dynamics which are needed for our main work.

Definition 2.1.1 (Fluid)

“A fluid is a substance that deforms continuously under the application of a shear (tangential) stress no matter how small the shear stress may be.” [44]

Definition 2.1.2 (Fluid Mechanics)

“Fluid mechanics is defined as science that deals with the behavior of fluids at rest (fluid statics) or in motion (fluid dynamics), and the interaction of fluids with

solid or other fluids at the boundaries.” [45]

Definition 2.1.3 (Fluid Dynamics)

“The study of fluid if the pressure forces are also considered for the fluids in motion, the branch of science is called fluid dynamics.” [45]

Definition 2.1.4 (Fluid Statics)

“The study of fluid at rest is called fluid statics.” [45]

Definition 2.1.5 (Viscosity)

“Viscosity is defined as the property of a fluid which offers resistance to the movement of one layer of fluid over another adjacent layer of the fluid.” [45] Mathematically,

$$\mu = \frac{\tau}{\frac{\partial u}{\partial y}},$$

where μ is viscosity coefficient, τ is shear stress and $\frac{\partial u}{\partial y}$ represents the velocity gradient. SI units of viscosity is $\frac{Ns}{m^2}$.

Definition 2.1.6 (Kinematic Viscosity)

“It is defined as the ratio between the dynamic viscosity and density of fluid. It is denoted by symbol ν called **nu**.” [45] Mathematically,

$$\nu = \frac{\mu}{\rho}.$$

SI unit of Kinematic Viscosity is m^2s^{-1} .

Definition 2.1.7 (Thermal Conductivity)

“The Fourier heat conduction law states that the heat flow is proportional to the temperature gradient. The coefficient of proportionality is a material parameter known as the thermal conductivity which may be a function of a number of variables.” [46] Mathematically,

$$q = -K\nabla T,$$

where K stands for the second order conductivity tensor. The form of K for an isotropic material is as follows:

$$K = kI,$$

where k denotes the thermal conductivity $[W/(m.C)]$ of the medium, and I is again the unit tensor.

Definition 2.1.8 (Magnetohydrodynamics)

“Magnetohydrodynamics (MHD) is concerned with the mutual interaction of fluid flow and magnetic fields. The fluids in question must be electrically conducting and non-magnetic, which limits us to liquid metals, hot ionised gases (plasmas) and strong electrolytes.” [47]

Definition 2.1.9 (Porosity)

“The porosity is the relationship of the volume of void space to the bulk volume of a permeable medium. A permeable medium is often identified by its porosity.” [48]

2.2 Types of Fluid

In this section, types of fluids are discussed which further help in understanding nature of fluid motion. The fluids may be classified into following four types.

Definition 2.2.1 (Ideal Fluid)

“A fluid, which is incompressible and has no viscosity, is known as an ideal fluid. Ideal fluid is only an imaginary fluid as all the fluids, which exist, have some viscosity.” [45]

Definition 2.2.2 (Real Fluid)

“A fluid which possesses viscosity is known as a real fluid. All the fluids in actual practice are real fluids.” [45]

Definition 2.2.3 (Newtonian Fluid)

“A real fluid, in which the shear stress is directly proportional to the rate of shear strain (or velocity gradient) is known as a Newtonian fluid. Mathematically, it can be written as:

$$\begin{aligned}\tau_{xy} &\propto \left(\frac{du}{dy}\right), \\ \tau_{xy} &= \mu \left(\frac{du}{dy}\right),\end{aligned}$$

where

μ = Dynamic viscosity, τ_{xy} = Shear stress exerted by the fluid, and $\frac{du}{dy}$ = Velocity gradient perpendicular to the direction of the shear.” [45]

Water and alcohol etc, are the common examples of Newtonian fluid.

Definition 2.2.4 (Non-Newtonian Fluid)

“A real fluid in which the shear stress is not directly proportional to the rate of shear strain (or velocity gradient), is known as a non-Newtonian fluid.” [45]

Mathematical, it can be expressed as:

$$\begin{aligned}\tau_{xy} &\propto k \left(\frac{du}{dy}\right)^m, \quad m \neq 1 \\ \tau_{xy} &= k \left(\frac{du}{dy}\right)^m,\end{aligned}$$

where

k is the flow consistency coefficient, $\frac{du}{dy}$ is shear rate, and n is the flow behaviour index.

Some examples of non-Newtonian fluids are toothpaste, shampoo, and honey etc.

Definition 2.2.5 (Ideal Plastic Fluid)

“A fluid, in which shear stress is more than the yield value and shear stress is

proportional to the rate of shear strain (or velocity gradient) is known as ideal plastic fluid.” [45]

For example blood and soap solution etc.

2.3 Types of Fluid Flow

Fluid flow is studied in fluid Mechanics and deals with fluid dynamics. This section gives the following eight types of fluid flow.

Definition 2.3.1 (Rotational Flow)

“Rotational flow is that type of flow in which the fluid particles while flowing along stream-lines, also rotate about their own axis.” [45]

Definition 2.3.2 (Irrotational Flow)

“Irrotational flow is that type of flow in which the fluid particles while flowing along stream-lines, do not rotate about their own axis then this type of flow is called irrotational flow.” [45]

Definition 2.3.3 (Compressible Flow)

“Compressible flow is that type of flow in which the density of the fluid changes from point to point or in other words the density (ρ) is not constant for the fluid.” [45] Mathematically,

$$\rho \neq k,$$

where k is constant.

Definition 2.3.4 (Incompressible Flow)

“Incompressible flow is that type of flow in which the density is constant for the fluid. Liquids are generally incompressible while gases are compressible.” [45] Mathematically,

$$\rho = k,$$

where k is constant.

Definition 2.3.5 (Steady Flow)

“If the flow characteristics such as depth of flow, velocity of flow, rate of flow at any point in open channel flow do not change with respect to time, the flow is said to be steady flow.” [49] Mathematically,

$$\frac{\partial Q}{\partial t} = 0,$$

where Q is any fluid property.

Flow of water through the nozzle of a garden hose illustrates that fluid particles may accelerate, even in a steady flow. In this example, the exit speed of the water is much higher than the water speed in the hose, implying that fluid particles have accelerated even though the flow is steady.

Definition 2.3.6 (Unsteady Flow)

“If at any point in open channel flow, the velocity of flow, depth of flow or rate of flow changes with respect to time, the flow is said to be unsteady.” [49] Mathematically,

$$\frac{\partial Q}{\partial t} \neq 0,$$

where Q is any fluid property.

When a rocket engine is fired up, for example, there are transient effects (the pressure builds up inside the rocket engine, the flow accelerates, etc.) until the engine settles down and operates steadily. The term periodic refers to the kind of unsteady flow in which the flow oscillates about a steady mean.

Definition 2.3.7 (Internal Flow)

“Flows completely bounded by a solid surfaces are called internal or duct flows. The examples of the internal flow are the flow through pipes or glass.” [44]

Definition 2.3.8 (External Flow)

“Flows over bodies immersed in an unbounded fluid are said to be an external flow. The flow of water in the ocean or in the river is an example of the external flow.” [44]

2.4 Modes of Heat Transfer

“In the field of engineering known as heat transfer, thermal energy is transferred from one point to another inside a medium or from one medium to another as a result of temperature differences. Different mechanisms are used for heat transfer.”

Definition 2.4.1 (Conduction)

“The transfer of heat within a medium due to a diffusion process is called conduction.” [46]

For example: When a car is started, the engine heats up, conduction can be seen in a radiator.

Definition 2.4.2 (Convection)

“Convection heat transfer is usually defined as energy transport effected by the motion of a fluid. The convection heat transfer between two dissimilar media is governed by Newtons law of cooling.” [46]

For example a cup of hot tea. The steam of heat transferred into the air.

Definition 2.4.3 (Thermal Radiation)

“The process by which heat is transferred from a body by virtue of its temperature, without the aid of any intervening medium, is called thermal radiation. Sometimes radiant energy is taken to be transported by electromagnetic waves while at other times it is supposed to be transported by particle like photons. Radiation is found to travel at the speed of light in vacuum. The term electromagnetic radiation encompasses many types of radiation such as:

- (i) Short wave radiation like gamma rays, x-rays and microwave.
- (ii) Long wave radiation like radio wave and thermal radiation. The cause for the

emission of each type of radiation is different. Thermal radiation is emitted by a medium due to its temperature.” [46]

Definition 2.4.4 (Viscous Dissipation)

“The irreversible process by means of which the work done by a fluid on adjacent layers due to the action of shear forces is transformed into heat is defined as viscous dissipation.” [39]

Definition 2.4.5 (Darcy-Forchheimer)

“The DarcyForchheimer (DF) model is probably the most popular modification to Darcian flow utilized in similarity inertia effects. Inertia effect is accounted through the inclusion of a velocity squared term in the momentum equation, which is known as Forchheimer’s extension.” [41]

2.5 Dimensionless Numbers

The following dimensionless number will appear in the discussion given in next chapters.

Definition 2.5.1 (Prandtl Number)

“It is the ratio between the momentum diffusivity ν and thermal diffusivity α . Mathematically, it can be defined as

$$Pr = \frac{\nu}{\alpha} = \frac{\frac{\mu}{\rho}}{\frac{k}{C_p \rho}} = \frac{\mu C_p}{k},$$

where μ represents the dynamic viscosity, C_p denotes the specific heat and k stands for thermal conductivity. The relative thickness of thermal and momentum boundary layer is controlled by Prandtl number.” [44]

Small prandtl values allow fluids to flow freely after those with high thermal conductivity, making them a suitable option for heat-conducting fluids.

Definition 2.5.2 (Skin Friction Coefficient)

“It expresses the dynamic friction resistance originating in viscous fluid flow around a fixed wall. The skin friction coefficient can be defined as

$$C_f = \frac{2\tau_w}{\rho U_w^2},$$

where τ_w denotes the shear stress on the wall, ρ the density and U_w the free-stream velocity.” [50]

Definition 2.5.3 (Nusselt Number)

“It is the relationship between the convective to the conductive heat transfer through the boundary of the surface. It is a dimensionless number which was first introduced by the German mathematician Nusselt. Mathematically, it is defined as:

$$Nu = \frac{qL}{k},$$

where q stands for convective heat transfer, L stands for characteristics length and k stands for thermal conductivity.” [50]

Definition 2.5.4 (Schmidt Number)

“Schmidt number (Sc) is a dimensionless number after Ernst Wilhelm Schmidt and characterized as the proportion of momentum diffusivity (viscosity) to mass diffusivity and is utilized to describe fluid flows in which there are simultaneous momentum and mass diffusion convection.” [50]

Definition 2.5.5 (Brownian diffusion coefficient)

“Brownian diffusion occurs due to the continuous collision between the molecules and nanoparticles of the fluid. It is denoted by D_B and is given by

$$D_B = \frac{K_B T C_c}{3\pi d \mu},$$

where K_B , T , C_c , and μ represents Boltzmann constant, temperature, correction factor and viscosity respectively stands for kinematic viscosity.” [51]

Definition 2.5.6 (Thermophoresis diffusion coefficient)

“The diffusion of particles is accelerated by the temperature gradient, which causes thermophoresis. It is denoted by D_T and is given by

$$D_T = \frac{-u_{th}T}{\nu\nabla T},$$

where u_{th} , T , ν and ∇T denote the thermophoretic velocity, temperature, kinematic viscosity and temperature gradient respectively.” [52]

2.6 Governing Laws

Definition 2.6.1 (Laws of Conservation of mass)

“The principle of conservation of mass can be stated as the time rate of change of mass in fixed volume is equal to the net rate of flow of mass across the surface. Mathematically, it can be written as

$$\frac{\partial \rho}{\partial t} + \nabla \cdot (\rho \mathbf{u}) = 0,$$

where ρ is the density kgm^{-3} of the medium, v the velocity vector ms^{-1} , and ∇ is the nabla or del operator. The continuity equation is in conservation (or divergence) form since it can be derived directly from an integral statement of mass conservation.” [46]

Definition 2.6.2 (Momentum Equation)

“The momentum equation states that the time rate of change of linear momentum of a given set of particles is equal to the vector sum of all the external forces acting on the particles of the set, provided Newtons third law of action and reaction governs the internal forces.” [46] Mathematically, it can be written as:

$$\frac{\partial}{\partial t}(\rho \mathbf{u}) + \nabla \cdot [(\rho \mathbf{u})\mathbf{u}] = \nabla \cdot \mathbf{T} + \rho g,$$

The above equation is called momentum equation.

Definition 2.6.3 (Energy Equation)

“The law of conservation of energy states that the time rate of change of the total energy is equal to the sum of the rate of work done by the applied forces and change of heat content per unit time.

$$\frac{\partial \rho}{\partial t} + \nabla \cdot \rho \mathbf{u} = -\nabla \cdot \mathbf{q} + Q + \phi,$$

where ϕ is the dissipation function.” [46]

2.7 Shooting Method

The boundary value problem that results from the main governing equation is solved using the shooting method. To elaborate the shooting method, consider the following nonlinear boundary value problem.

$$\left. \begin{aligned} f''(x) &= f(x)f'(x) + 2f^2(x) \\ f(0) &= 0, \quad f(L) = J. \end{aligned} \right\} \quad (2.1)$$

To reduce the order of the above boundary value problem, introduce the following notations.

$$f = Y_1, \quad f' = Y_1' = Y_2, \quad f'' = Y_2'. \quad (2.2)$$

As a result, (2.1) is converted into the following system of first order ODEs.

$$Y_1' = Y_2, \quad Y_1(0) = 0, \quad (2.3)$$

$$Y_2' = Y_1 Y_2 + 2Y_1^2, \quad Y_2(0) = u. \quad (2.4)$$

where u is the missing initial condition which will found by using the Newton method. The above IVP will be numerically solved by the order-4 Runge-Kutta

method. The missing condition u is to be chosen such that.

$$Y_1(L, u) = J. \quad (2.5)$$

For convenience, now onward $Y_1(L, u)$ will be denoted by $Y_1(u)$.

Let us further denote $Y_1(u) - J$ by $H(u)$, so that (2.5) becomes.

$$H(u) = 0. \quad (2.6)$$

The above equation can be solved by using Newton's method with the following iterative formula.

$$u^{n+1} = u^n - \frac{H(u^n)}{\frac{\partial H(u^n)}{\partial u}}, \quad n = 0, 1, 2, 3, \dots$$

or

$$u^{n+1} = u^n - \frac{Y_1(u^n) - J}{\frac{\partial Y_1(u^n)}{\partial u}}, \quad n = 0, 1, 2, 3, \dots \quad (2.7)$$

To find $\frac{\partial Y_1(u^n)}{\partial u}$, introduce the following notations.

$$\frac{\partial Y_1}{\partial u} = Y_3, \quad \frac{\partial Y_2}{\partial u} = Y_4. \quad (2.8)$$

As a result of above new notations the Newton's iterative scheme, will then get the form.

$$u^1 = u^0 - \frac{Y_1(u) - J}{Y_3(u)}. \quad (2.9)$$

Now differentiating (2.3) and (2.4) with respect to u , we get the following two equations.

$$Y_3' = Y_4, \quad Y_3(0) = 0. \quad (2.10)$$

$$Y_4' = Y_3Y_2 + Y_1Y_4 + 4Y_1Y_3, \quad Y_4(0) = 1. \quad (2.11)$$

Writing all the four ODEs (2.3), (2.4), (2.10) and (2.11) together, we have the following initial value problem.

$$Y_1' = Y_2, \quad Y_1(0) = 0.$$

$$Y_2' = Y_1Y_2 + 2Y_1^2, \quad Y_2(0) = u.$$

$$Y_3' = Y_4, \quad Y_3(0) = 0.$$

$$Y_4' = Y_3Y_2 + Y_1Y_4 + 4Y_1Y_3, \quad Y_4(0) = 1.$$

The above system will be solved numerically by Runge-Kutta method of order four. The stopping criteria for the Newton's technique is set as,

$$|Y_1(u) - J| < \epsilon,$$

where $\epsilon > 0$ is an arbitrarily small positive number.

Chapter 3

Darcy-Forchheimer Nanofluid Flow between Horizontal Plates

3.1 Introduction

In this chapter, consideration has been given to the numerical analysis of the MHD and nanofluid flow in a Darcy-Forchheimer medium between two horizontal plates. The lower plate's normal direction involves a uniformly produced magnetic impact. The governing nonlinear PDEs are converted into a system of dimensionless ODEs by utilizing the appropriate transformations. In order to solve the ODEs, the shooting technique is implemented in MATLAB. At the end of this chapter the numerical solution for various parameters is discussed for the dimensionless velocity profile $f'(\eta)$ and temperature distribution $\theta(\eta)$. Investigation of obtained numerical results are given through graphs. This chapter provides a detailed review of the work presented by Rasool et al. [1]

3.2 Mathematical Modeling

Consider a steady squeezed nanofluid flow contained between two horizontally adjusted h -distance apart plates. The location of plates is fixed $x_2 = 0$ at one side and $x_2 = h$ at the other side in Cartesian coordinates. The bottom plate is stretched with at the rate of $u_1 = zx_1$, where z is a positive constant integer. A uniformly induced magnetic impact is involved in the normal direction to the lower plate. Darcy-Forchheimer medium is considered between the plates, it allows horizontal axis flow with the help of friction and porosity effects. Figure 3.1 depicts the geometry of the flow.

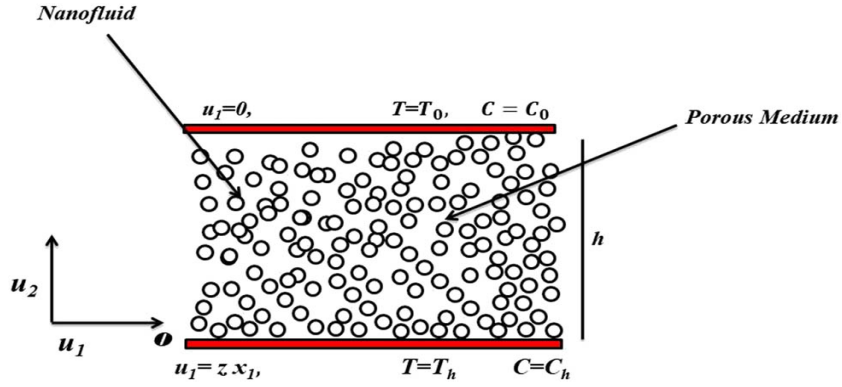


FIGURE 3.1: Geometry of the problem.

The governing equations are taken from [1] as:

Continuity Equation:

$$\frac{\partial u_1}{\partial x_1} + \frac{\partial u_2}{\partial x_2} = 0, \quad (3.1)$$

Momentum Equations:

$$u_1 \frac{\partial u_1}{\partial x_1} + u_2 \frac{\partial u_1}{\partial x_2} = -\frac{1}{\rho_f} \frac{\partial p}{\partial x_1} + \nu \left(\frac{\partial^2 u_1}{\partial x_1^2} + \frac{\partial^2 u_1}{\partial x_2^2} \right) - \frac{\sigma B_0^2}{\rho_f} u_1 - \frac{\nu}{K} u_1 - F u_1^2, \quad (3.2)$$

$$u_1 \frac{\partial u_2}{\partial x_1} + u_2 \frac{\partial u_2}{\partial x_2} = -\frac{1}{\rho_f} \frac{\partial p}{\partial x_2} + \nu \left(\frac{\partial^2 u_2}{\partial x_1^2} + \frac{\partial^2 u_2}{\partial x_2^2} \right), \quad (3.3)$$

Energy Equation:

$$u_1 \frac{\partial T}{\partial x_1} + u_2 \frac{\partial T}{\partial x_2} = \alpha \left(\frac{\partial^2 T}{\partial x_1^2} + \frac{\partial^2 T}{\partial x_2^2} \right) + \tau \left(D_B \left(\frac{\partial C}{\partial x_2} \frac{\partial T}{\partial x_2} + \frac{\partial C}{\partial x_1} \frac{\partial T}{\partial x_1} \right) + \frac{D_T}{T_h} \left(\frac{\partial T}{\partial x_1} \right)^2 + \left(\frac{\partial T}{\partial x_2} \right)^2 \right), \quad (3.4)$$

$$u_1 \frac{\partial C}{\partial x_1} + u_2 \frac{\partial C}{\partial x_2} = D_B \left(\frac{\partial^2 C}{\partial x_1^2} + \frac{\partial^2 C}{\partial x_2^2} \right) + \frac{D_T}{T_h} \left(\frac{\partial^2 T}{\partial x_1^2} + \frac{\partial^2 T}{\partial x_2^2} \right), \quad (3.5)$$

where D_B is the Brownian diffusion, D_T is the Thermophoretic diffusion, ν is Kinematic viscosity, α is Thermal diffusivity, and B_0 is the Magnetic number.

The associated BCs given as.

$$\left. \begin{aligned} u_1 = u_w = zx_1, \quad u_2 = 0, \quad C = C_h, \quad T = T_h, \quad \text{at } x_2 = 0, \\ u_1 = 0, \quad C = C_0, \quad T = T_0, \quad \text{at } x_2 = +h. \end{aligned} \right\} \quad (3.6)$$

As a first step the pressure term is eliminated from (3.2) and (3.3).

$$\begin{aligned} & \frac{\partial u_1}{\partial x_1} \frac{\partial u_1}{\partial x_2} + u_1 \frac{\partial^2 u_1}{\partial x_1 \partial x_2} + \frac{\partial u_1}{\partial x_2} \frac{\partial u_2}{\partial x_2} + u_2 \frac{\partial^2 u_1}{\partial x_2^2} - \frac{\partial u_1}{\partial x_1} \frac{\partial u_2}{\partial x_1} - u_1 \frac{\partial^2 u_2}{\partial x_1^2} - \frac{\partial u_2}{\partial x_1} \frac{\partial u_2}{\partial x_2} \\ & - u_2 \frac{\partial^2 u_2}{\partial x_1 \partial x_2} = \nu \left(\frac{\partial^3 u_1}{\partial x_1^2 \partial x_2} + \frac{\partial^3 u_1}{\partial x_2^3} - \frac{\partial^3 u_2}{\partial x_2^2 \partial x_1} - \frac{\partial^3 u_2}{\partial x_1^3} \right) - \frac{\sigma B_0^2}{\rho_f} \frac{\partial u_1}{\partial x_2} \\ & - \frac{\nu}{K} \frac{\partial u_1}{\partial x_2} - 2Fu_1 \frac{\partial u_1}{\partial x_2}. \end{aligned} \quad (3.7)$$

To convert derivatives, use the following transformation:

$$\left. \begin{aligned} u_1 = zx_1 \frac{\partial f}{\partial \eta}, \quad u_2 = -zhf, \quad \eta = \frac{x_2}{h}, \\ (T_0 - T_h) \theta(\eta) = (T - T_h), \\ (C_0 - C_h) \theta(\eta) = (C - C_h). \end{aligned} \right\} \quad (3.8)$$

Continuity equation is trivially satisfied as follows:

$$\begin{aligned}\frac{\partial u_1}{\partial x_1} + \frac{\partial u_2}{\partial x_2} &= z f' - z f', \\ \frac{\partial u_1}{\partial x_1} + \frac{\partial u_2}{\partial x_2} &= 0.\end{aligned}$$

Some important derivatives are calculated as follows:

- $\frac{\partial u_1}{\partial x_1} = z f'$,
- $\frac{\partial^2 u_1}{\partial x_1^2} = 0$,
- $\frac{\partial^2 u_2}{\partial x_2^2} = -\frac{1}{h} z f''$,
- $\frac{\partial u_1}{\partial x_2} = \frac{\partial}{\partial x_2}(z x_1)$,
- $\frac{\partial u_2}{\partial x_1} = 0$,
- $\frac{\partial u_2}{\partial x_2} = \frac{z x_1 f''}{h}$,
- $\frac{\partial u_2}{\partial x_2} = -z f'$,
- $\frac{\partial^2 u_2}{\partial x_1^2} = 0$,
- $\frac{\partial^2 u_1}{\partial x_1 \partial x_2} = \frac{z f''}{h}$,
- $\frac{\partial^2 u_2}{\partial x_1 \partial x_2} = 0$,
- $\frac{\partial^3 u_1}{\partial x_2 \partial x_1^2} = 0$,
- $\frac{\partial^3 u_1}{\partial x_2^3} = \frac{z x_1 f^{iv}}{h^3}$,
- $\frac{\partial^2 u_1}{\partial x_2^2} = \frac{z x_1 f''' }{h^2}$,
- $\frac{\partial^3 u_2}{\partial x_1^3} = 0$,
- $\frac{\partial^3 u_2}{\partial x_1 \partial x_2^2} = 0$.

The above derivatives are plugged into (3.7), to get:

$$\begin{aligned}
 & (zx_1 f') \left(\frac{z}{h} f'' \right) + (z f') \left(\frac{zx_1}{h} f''' \right) + (-zhf) \left(\frac{zx_1}{h^2} f'''' \right) + (-zf') \left(\frac{zx_1}{h} f'' \right) \\
 & - (zx_1 f')(0) - (zf')(0) - (-zhf)(0) - (-zf')(0) = \nu \left(\frac{zx_1}{h^3} f^{iv} \right) \\
 & - \frac{\sigma B_0^2}{\rho_f} \frac{zx_1}{h} f'' - \frac{\nu}{k} \frac{zx_1}{h} f'' - 2F(zx_1 f') \frac{zx_1}{h} f'', \\
 \Rightarrow & \frac{z^2 x_1}{h} f' f'' + \frac{z^2 x_1}{h} f' f'' - \frac{z^2 x_1}{h} f' f''' - \frac{z^2 x_1}{h} f' f'' = \frac{\nu z x_1}{h^3} f^{iv} - \frac{\sigma B_0^2}{\rho_f} \frac{zx_1}{h} f'' \\
 & - \frac{\nu}{k} \frac{zx_1}{h} f'' - \frac{2F z^2 x_1^2}{h} f' f'', \\
 \Rightarrow & \frac{z^2 x_1}{h} f' f'' - \frac{z^2 x_1}{h} f' f''' = \frac{\nu z x_1}{h^3} f^{iv} - \frac{\sigma B_0^2}{\rho_f} \frac{zx_1}{h} f'' - \frac{\nu}{k} \frac{zx_1}{h} f'' - \frac{2F z^2 x_1^2}{h} f' f'', \\
 & \frac{\nu z x_1}{h^3} f^{iv} - \frac{z^2 x_1}{h} f' f'' + \frac{z^2 x_1}{h} f' f''' - \frac{\sigma B_0^2}{\rho_f} \frac{zx_1}{h} f'' - \frac{\nu}{k} \frac{zx_1}{h} f'' - \frac{2F z^2 x_1^2}{h} f' f'' = 0,
 \end{aligned} \tag{3.9}$$

Multiplying (3.9) with $\frac{h^3}{\nu z x_1}$.

$$\begin{aligned}
 & \left(\frac{h^3}{\nu z x_1} \right) \left(\frac{\nu z x_1}{h^3} \right) f^{iv} - \left(\frac{h^3}{\nu z x_1} \right) \left(\frac{z^2 x_1}{h} \right) [f' f'' - f f'''] - \left(\frac{h^3}{\nu z x_1} \right) \left(\frac{\sigma B_0^2 z x_1}{\rho_f k} \right) f'' \\
 & - \left(\frac{h^3}{\nu z x_1} \right) \left(\frac{\nu z x_1}{k h} \right) f'' - \left(\frac{h^3}{\nu z x_1} \right) \left(\frac{2F z^2 x_1^2}{h} \right) f' f'' = 0, \\
 & f^{iv} - \frac{h^2 z}{\nu} (f' f'' - f f''') - \frac{\sigma B_0^2 h^2}{\rho_f \nu} f'' - \frac{h^2}{k} f'' - \frac{2F z x_1 h^2}{\nu} f' f'' = 0, \\
 & P = \frac{h^2 z}{\nu}, \quad M = \frac{\sigma B_0^2 h^2}{\rho_f \nu}, \quad \lambda = \frac{h^2}{k}, \quad F_r = \frac{F z h x_1}{\nu}, \\
 & f^{iv} - P(f' f'' - f f''') - M f'' - \lambda f'' - 2h F_r f' f'' = 0.
 \end{aligned}$$

For the conversion of the temperature equation (3.4) into an ordinary differential equation. The following derivatives are evaluated:

$$u_1 = z x_1 \frac{\partial f}{\partial \eta}, \quad u_2 = -zhf, \quad \eta = \frac{x_2}{h},$$

- $(T_0 - T_h)\theta(\eta) = (T - T_h),$
- $(C_0 - C_h)\phi(\eta) = (C - C_h),$
- $\frac{\partial T}{\partial x_1} = 0,$
- $\frac{\partial^2 T}{\partial x_1^2} = 0,$
- $\frac{\partial C}{\partial x_1} = 0,$
- $\frac{\partial^2 C}{\partial x_1^2} = 0,$
- $\frac{\partial T}{\partial x_2} = \frac{(T_0 - T_h)}{h}\theta'(\eta),$
- $\frac{\partial C}{\partial x_2} = \frac{(C_0 - C_h)}{h}\phi'(\eta),$
- $\frac{\partial^2 T}{\partial x_2^2} = \frac{(T_0 - T_h)}{h^2}\theta''(\eta),$
- $\frac{\partial^2 C}{\partial x_2^2} = \frac{(C_0 - C_h)}{h^2}\phi''(\eta),$
- $\left(\frac{\partial T}{\partial x_2}\right)^2 = \frac{(T_0 - T_h)^2}{h^2}\theta'^2.$

Using all of the derivatives calculated above in (3.4), to get:

$$\begin{aligned}
\Rightarrow \quad & u_1 \frac{\partial T}{\partial x_1} + u_2 \frac{\partial T}{\partial x_2} = \alpha \left(\frac{\partial^2 T}{\partial x_1^2} + \frac{\partial^2 T}{\partial x_2^2} \right) + \tau \left(D_B \left(\frac{\partial C}{\partial x_2} \frac{\partial T}{\partial x_2} + \frac{\partial C}{\partial x_1} \frac{\partial T}{\partial x_1} \right) \right. \\
& \left. + \frac{D_T}{T_h} \left(\frac{\partial T}{\partial x_1} \right)^2 + \left(\frac{\partial T}{\partial x_2} \right)^2 \right), \\
\Rightarrow \quad & + z x_1 f'(0) + (-z h f) \frac{T_0 - T_h}{h} \theta' = \alpha \left(\frac{(T_0 - T_h)}{h^2} \theta'' \right), \\
& + \tau \left[D_B \left(\frac{(T_0 - T_h)}{h} \theta' \frac{C_0 - C_h}{h} \phi' \right) + \frac{D_T}{h} \left(\frac{(T_0 - T_h)^2}{h^2} \theta'^2 \right) \right], \\
\Rightarrow \quad & - z f (T_0 - T_h) \theta' = \alpha \frac{(T_0 - T_h)}{h^2} \theta'' + \tau D_B \frac{(T_0 - T_h)(C_0 - C_h)}{h^2} \theta' \phi', \\
& + \tau \frac{D_T}{T_h} \frac{(T_0 - T_h)^2}{h^2} \theta'^2, \\
\Rightarrow \quad & \theta'' + \frac{h_2}{\alpha(T_0 - T_h)} \frac{\tau D_B (T_0 - T_h)(C_0 - C_h)}{h^2} \theta' \phi' + \frac{h_2}{\alpha(T_0 - T_h)} z f (T_0 - T_h) \theta', \\
& + \frac{h_2}{\alpha(T_0 - T_h)} \frac{\tau D_T}{T_h} \frac{(T_0 - T_h)^2}{h^2} \theta'^2 = 0,
\end{aligned}$$

$$\begin{aligned} \Rightarrow \quad & \theta'' + \frac{\tau D_B(C_0 - C_h)h^2}{\alpha} \theta' \phi' + \frac{h^2 z f}{\alpha} \theta' + \frac{\tau D_T(T_0 - T_h)^2}{T_h \alpha} \theta'^2 = 0, \\ & N_t = \frac{\tau D_T(T_0 - T_h)}{\alpha T_h}, \quad N_b = \frac{\tau D_B(C_0 - C_h)}{\alpha}, \\ & P = \frac{h^2 z}{v}, \quad P_r = \frac{v}{\alpha}, \\ & \theta'' + N_b \theta' \phi' + \frac{h^2 z}{v} P_r f \theta' + N_t \theta'^2 = 0, \\ & \theta'' + N_b \theta' \phi' + P P_r f \theta' + N_t \theta'^2 = 0. \\ & u_1 = z x_1 \frac{\partial f}{\partial \eta}, \quad u_2 = -z h f, \quad \eta = \frac{x_2}{h}, \end{aligned}$$

For the conversion of equation (3.5) into an ordinary differential equation. The following derivatives are evaluated:

- $\frac{\partial C}{\partial x_1} = 0,$
- $\frac{\partial C}{\partial x_2} = \frac{(C_0 - C_h)}{h} \phi'(\eta),$
- $\frac{\partial^2 C}{\partial x_1^2} = 0,$
- $\frac{\partial^2 C}{\partial x_2^2} = \frac{(C_0 - C_h)}{h^2} \phi''(\eta),$
- $\frac{\partial^2 T}{\partial x_1^2} = 0,$
- $\frac{\partial^2 T}{\partial x_2^2} = \frac{(T_0 - T_h)}{h^2} \theta''(\eta).$

The above values use in equation (3.5),

$$\begin{aligned} u_1 \frac{\partial C}{\partial x_1} + u_2 \frac{\partial C}{\partial x_2} &= D_B \left(\frac{\partial^2 C}{\partial x_1^2} + \frac{\partial^2 C}{\partial x_2^2} \right) + \frac{D_T}{T_h} \left(\frac{\partial^2 T}{\partial x_1^2} + \frac{\partial^2 T}{\partial x_2^2} \right), \\ (-z h f) \frac{(C_0 - C_h)}{h} \phi' &= D_B \left(\frac{(C_0 - C_h)}{h^2} \phi'' \right) + \frac{D_T}{T_h} \left(\frac{(T_0 - T_h)}{h^2} \theta'' \right), \\ -z f (C_0 - C_h) \phi' &= \frac{D_B (C_0 - C_h)}{h^2} \phi'' + \frac{D_T (T_0 - T_h)}{T_h h^2} \theta'', \\ \frac{D_B (C_0 - C_h)}{h^2} \phi'' + z f (C_0 - C_h) \phi' + \frac{D_T (T_0 - T_h)}{T_h h^2} \theta'' &= 0, \\ \phi'' + \frac{z h^2 f (C_0 - C_h)}{D_B (C_0 - C_h)} \phi' + \frac{D_T h^2}{T_h D_B (C_0 - C_h)} \frac{(T_0 - T_h)}{h^2} \theta'' &= 0, \end{aligned}$$

$$\phi'' + \frac{zh_2v}{vD_B}f\phi' + \frac{\tau D_T(T_0 - T_h)}{\alpha T_h} \frac{1}{\frac{\tau D_B(C_0 - C_h)}{\alpha}} \theta'' = 0,$$

$$\phi'' + PS_c f \phi' + \frac{N_t}{N_b} \theta'' = 0.$$

Dimensionless Boundary Conditions:

- $u_1 = zx_1 \frac{\partial f}{\partial \eta}, \quad \text{at} \quad y = 0.$

$$u_1 = zx_1,$$

$$zx_1 \frac{\partial f}{\partial \eta} = zx_1,$$

$$\frac{\partial f}{\partial \eta} = 1,$$

$$f' = 1, \quad \text{at} \quad \eta = 0.$$

- $u_2 = -zhf, \quad \text{at} \quad y = 0.$

$$u_2 = 0,$$

$$-zhf = 0,$$

$$f = 0.$$

- $(T_0 - T_h) \theta(\eta) = (T - T_h),$

$$\theta(\eta) = \frac{T - T_h}{T_0 - T_h},$$

$$T = T_0,$$

$$\theta(\eta) = \frac{T_0 - T_h}{T_0 - T_h},$$

$$\theta(\eta) = 1.$$

- $(C_0 - C_h) \phi(\eta) = (C - C_h),$

$$\phi(\eta) = \frac{C - C_h}{C_0 - C_h},$$

$$C = C_0,$$

$$\phi(\eta) = \frac{C_0 - C_h}{C_0 - C_h},$$

$$\phi(\eta) = 1.$$

- $u_1 = zx_1 \frac{\partial f}{\partial \eta}, \quad \text{at} \quad y = 1.$

$$u_1 = 0,$$

$$zx_1 \frac{\partial f}{\partial \eta} = 0,$$

$$\frac{\partial f}{\partial \eta} = 0,$$

$$f' = 0, \quad \text{at} \quad \eta = 1.$$

- $u_2 = -zhf, \quad \text{at} \quad y = 1.$

$$u_2 = 0,$$

$$-zhf = 0,$$

$$f = 0.$$

- $(T_0 - T_h)\theta(\eta) = (T - T_h),$

$$\theta(\eta) = \frac{T - T_h}{T_0 - T_h},$$

$$T = T_h,$$

$$\theta(\eta) = \frac{T_h - T_h}{T_0 - T_h},$$

$$\theta(\eta) = 0.$$

- $(C_0 - C_h)\phi(\eta) = (C - C_h),$

$$\phi(\eta) = \frac{C - C_h}{C_0 - C_h},$$

$$C = C_h,$$

$$\phi(\eta) = \frac{C_h - C_h}{C_0 - C_h},$$

$$\phi(\eta) = 0.$$

Finally, the following ordinary differential equations are obtained:

$$f^{iv} - P(f'f'' - ff''') - Mf'' - \lambda f'' - 2hF_r f'f'' = 0, \quad (3.10)$$

$$\theta'' + N_b \theta' \phi' + PP_r f \theta' + N_t \theta'^2 = 0, \quad (3.11)$$

$$\phi'' + PS_c f \phi' + \frac{N_t}{N_b} \theta'' = 0. \quad (3.12)$$

with the boundary conditions:

$$\left. \begin{aligned} f = 0, \quad f' = 1, \quad \theta = 1 = \phi, \quad \text{at } \eta = 0, \\ f = 0, \quad f' = 0, \quad \theta = 0 = \phi, \quad \text{at } \eta = 1, \end{aligned} \right\} \quad (3.13)$$

where $P = \frac{h^2 z}{\nu}$ is the viscosity parameter, $\lambda = \frac{h^2}{k}$ is the porosity, $F_r = \frac{Fz hx_1}{\nu}$ is the Forchheimer number such that $F = \frac{C_b}{\sqrt{K}}$ is the drag force coefficient and $M = \frac{\sigma B_0^2 h^2}{\rho_f \nu}$ is the magnetic parameter.

In the energy equation, $Pr = \frac{\nu}{\alpha}$ is the Prandtl factor, $N_b = \frac{\tau D_B (C_0 - C_h)}{\alpha}$ is the Brownian motion factor, $N_t = \frac{\tau D_T (T_0 - T_h)}{\alpha T_h}$ is the thermophoresis factor, and $S_c = \frac{\nu}{D_B}$ is the Schmidt factor.

The physical quantities are given as:

$$\left(\frac{Px_1}{h} \right) C_f = f''(0),$$

$$Nu_x = \theta'(0).$$

3.3 Numerical Treatment

This section is dedicated to the implementation of the shooting method to solve the transformed ODEs (3.10) (3.11) and (3.12) subject to the boundary conditions (3.6). One can easily observe that (3.10) is independent of θ , and ϕ , so we will first find the solution of (3.10). For this purpose, the following notations are used:

$$f = y_1$$

$$f' = y_1' = y_2$$

$$f'' = y_2' = y_3$$

$$f''' = y_3' = y_4$$

$$f^{iv} = y_4'.$$

Utilizing the above notations, we have the following system of four first order differential equations.

$$\begin{aligned} y_1' &= y_2; & y_1(0) &= 0, & y_1(1) &= 0, \\ y_2' &= y_3; & y_2(0) &= 1, & y_2(1) &= 0, \\ y_3' &= y_4; & y_3(0) &= R, \\ y_4' &= P(y_2y_3 - y_1y_4) - My_3 - \lambda y_3 - 2F_r y_2y_3 = 0, & y_4(0) &= S, \end{aligned}$$

where R and S are assumed missing conditions. To solve the above system by using Runge Kutta method of order four, two missing initial conditions R and S are such that:

$$\begin{aligned} y_1(\eta, R, S)_{\eta=1} - 0 &= 0, \\ y_2(\eta, R, S)_{\eta=1} - 0 &= 0. \end{aligned}$$

Now

$$y_1(0) = y(0) = R, \quad y_2(0) = y'(0) = S.$$

The Newton's method is used to solve the above algebraic equation and has the following iterative scheme:

$$\begin{bmatrix} R^{n+1} \\ S^{n+1} \end{bmatrix} = \begin{bmatrix} R^n \\ S^n \end{bmatrix} - \begin{bmatrix} \frac{\partial y_1}{\partial R} & \frac{\partial y_1}{\partial S} \\ \frac{\partial y_2}{\partial R} & \frac{\partial y_2}{\partial S} \end{bmatrix}^{-1} \begin{bmatrix} y_1(1) - 0 \\ y_2(1) - 0 \end{bmatrix} \quad (3.14)$$

To incorporate the above formula, we further need the following derivatives:

$$\frac{\partial y_1}{\partial R} = y_5, \quad \frac{\partial y_2}{\partial R} = y_6, \quad \frac{\partial y_3}{\partial R} = y_7, \quad \frac{\partial y_4}{\partial R} = y_8,$$

$$\frac{\partial y_1}{\partial S} = y_9, \quad \frac{\partial y_2}{\partial S} = y_{10}, \quad \frac{\partial y_3}{\partial S} = y_{11}, \quad \frac{\partial y_4}{\partial S} = y_{12}.$$

As the result of these notations, the Newton's iterative scheme gets the form:

$$\begin{bmatrix} R^{n+1} \\ S^{n+1} \end{bmatrix} = \begin{bmatrix} R^n \\ S^n \end{bmatrix} - \begin{bmatrix} y_5 & y_9 \\ y_6 & y_{10} \end{bmatrix}^{-1} \begin{bmatrix} y_1(1) - 0 \\ y_2(1) - 0 \end{bmatrix} \quad (3.15)$$

Now differentiate the above system of four first order ODE's (3.14) with respect to each of the variables R and S to have another system of eight ODE's together, the following IVP has:

$$\begin{aligned} y_1' &= y_2; & y_1(0) &= 0, \\ y_2' &= y_3; & y_2(0) &= 0, \\ y_3' &= y_4; & y_3(0) &= R, \\ y_4' &= P(y_2y_3 - y_1y_4) - My_3 - \lambda y_3 - 2F_r y_2y_3; & y_4(0) &= S, \\ y_5' &= y_6; & y_5(0) &= 0, \\ y_6' &= y_7; & y_6(0) &= 0, \\ y_7' &= y_8; & y_7(0) &= 1, \\ y_8' &= P(y_3y_6 + y_2y_7 - y_4y_5 - y_1y_8) - My_7 - \lambda y_7 - 2F_r(y_3y_6 + y_2y_7); & y_8(0) &= 0, \\ y_9' &= y_{10}; & y_9(0) &= 0, \\ y_{10}' &= y_{11}; & y_{10}(0) &= 0, \\ y_{11}' &= y_{12}; & y_{11}(0) &= 0, \\ y_{12}' &= P(y_3y_{10} + y_2y_{11} - y_4y_9 - y_1y_{12}) - My_{11} - \lambda y_{11} \\ &\quad - 2F_r(y_3y_{10} + y_2y_7); & y_{12}(0) &= 1. \end{aligned}$$

The Runge Kutta method of order four is used to solve the above system of twelve first order differential equations with R and S as initial guess. The iterative process is repeated until the criteria listed below is met:

$$\max [|y_1(\eta, R, S)|, |y_2(\eta, R, S)|] < \epsilon,$$

for an arbitrarily small positive value of ϵ . Throughout this chapter ϵ has been taken as $(10)^{-6}$. Since (3.11) and (3.12) are coupled equations. So (3.12) will be

solved separately by incorporating the solution of (3.11). For this purpose let us denote:

$$\theta = Y_1, \quad \theta' = Y_1' = Y_2, \quad \theta'' = Y_2'$$

and

$$\phi = Y_3, \quad \phi' = Y_3' = Y_4, \quad \phi'' = Y_4' = Y_5$$

and

$$f = D.$$

to get the following first order ODE's.

$$\begin{aligned} Y_1' &= Y_2; & Y_1(0) &= 1, & Y_1(1) &= 0, \\ Y_2' &= -N_b Y_4 Y_2 - PP_r D Y_2 - N_t Y_2^2; & Y_2(0) &= R, \\ Y_3' &= Y_4; & Y_3(0) &= 1, & Y_3(1) &= 0, \\ Y_4' &= -PS_c D Y_4 - \frac{N_t}{N_b} Y_3; & Y_4(0) &= S, \end{aligned}$$

The above IVP is solved numerically by Runge Kutta method of order four. In the above initial value problem, the missing condition m is to be chosen such that:

$$\begin{aligned} Y_1(\eta, R, S)_{\eta=1} - 0 &= 0, \\ Y_3(\eta, R, S)_{\eta=1} - 0 &= 0. \end{aligned}$$

Now

$$Y_1(0) = Y(0) = R, \quad Y_2(0) = Y'(0) = S$$

The Newton's method is used to solve algebraic equations system and has the following iterative scheme:

$$\begin{bmatrix} R^{n+1} \\ S^{n+1} \end{bmatrix} = \begin{bmatrix} R^n \\ S^n \end{bmatrix} - \begin{bmatrix} \frac{\partial Y_1}{\partial R} & \frac{\partial Y_1}{\partial S} \\ \frac{\partial Y_3}{\partial R} & \frac{\partial Y_3}{\partial S} \end{bmatrix}^{-1} \begin{bmatrix} Y_1(1) - 0 \\ Y_3(1) - 0 \end{bmatrix} \quad (3.16)$$

To incorporate the above formula, we further need the following derivatives:

$$\begin{aligned}\frac{\partial Y_1}{\partial R} &= Y_5, & \frac{\partial Y_2}{\partial R} &= Y_6. \\ \frac{\partial Y_3}{\partial R} &= Y_7, & \frac{\partial Y_4}{\partial R} &= Y_8. \\ \frac{\partial Y_1}{\partial S} &= Y_9, & \frac{\partial Y_2}{\partial S} &= Y_{10}. \\ \frac{\partial Y_3}{\partial S} &= Y_{11}, & \frac{\partial Y_4}{\partial S} &= Y_{12}.\end{aligned}$$

As the result of these notations, the Newton's iterative scheme gets the form:

$$\begin{bmatrix} R^{n+1} \\ S^{n+1} \end{bmatrix} = \begin{bmatrix} R^n \\ S^n \end{bmatrix} - \begin{bmatrix} Y_5 & Y_9 \\ Y_7 & Y_{11} \end{bmatrix}^{-1} \begin{bmatrix} Y_1(1) - 0 \\ Y_3(1) - 0 \end{bmatrix} \quad (3.17)$$

Here n is the number of iterations ($n = 0, 1, 2, 3, 4, 5, \dots$).

Now differentiate the above system of four first order ODE's (3.16) with respect to each of the variables R and S to have another system of eight ODE's together, the initial condition:

$$\begin{aligned}Y_1' &= Y_2; & Y_1(0) &= 1, \\ Y_2' &= -N_b Y_4 Y_2 - PP_r DY_2 - N_t Y_2^2; & Y_2(0) &= R, \\ Y_3' &= Y_4; & Y_3(0) &= 1, \\ Y_4' &= -PS_c DY_4 - \frac{N_t}{N_b} Y_3; & Y_4(0) &= S, \\ Y_5' &= Y_6; & Y_7(0) &= 0, \\ Y_6' &= -N_b(Y_2 Y_8 + Y_4 Y_6) - PP_r DY_6 - 2N_t Y_2 Y_6; & Y_6(0) &= 1, \\ Y_7' &= Y_8; & Y_7(0) &= 0, \\ Y_8' &= -PS_c DY_8 - \frac{N_t}{N_b} Y_7; & Y_8(0) &= 0, \\ Y_9' &= Y_{10}; & Y_9(0) &= 0, \\ Y_{10}' &= -N_b(Y_2 Y_{12} + Y_4 Y_{10}) - PP_r DY_{10} - 2N_t Y_2 Y_{10}; & Y_{10}(0) &= 0, \\ Y_{11}' &= Y_{12}; & Y_{11}(0) &= 0, \\ Y_{12}' &= -PS_c DY_{12} - \frac{N_t}{N_b} Y_{11}; & Y_{12}(0) &= 1.\end{aligned}$$

The Runge Kutta method of order four is used to solve the above system of twelve first order differential equations with R and S initial guess. The iterative process is repeated until the criteria listed below are met:

$$\max [| Y_1(\eta, R, S) |, | Y_3(\eta, R, S) |] < \epsilon$$

for an arbitrarily small positive value of ϵ . Throughout this chapter ϵ was taken as $(10)^{-6}$.

3.4 Results and Discussions

This phase explores the graphical consequences and their bodily justifications for the three most important profiles that includes velocity, temperature and concentration of nanoparticles. Figures 3.2 to 3.18 are plotted to reveal the effects of numerous fluid parameters concerned in the present flow model.

Figures (3.2) and (3.3) are graphical description of the effect of Forchheimer parameter on velocity f and f' respectively. A closer view elaborates the velocity field decreases with increase in the Forchheimer number. Physically, the relation of Forchheimer coefficient with drag force coefficient is liable for this trend in velocity parameter. For greater Forchheimer number an intensive velocity field is observed which results in bigger amount of frictional force to the flow. Therefore, a decline is noticed in velocity profile.

Figures (3.4) and (3.5) shows the effect of magnetic field on fluid flow via Darcy Medium. The effect of magnetic field is inversely related to the flow of said fluid. Physically, a magnetic field which is normal to the surface creates collisions with direction of flow. Therefore, a decline is observed in both f and f' . Impact of viscosity parameter P on both f and f' is shown in Figures (3.6) and (3.7), respectively. Physically, for large values of P the inverse relation of kinematic viscosity confirms the enhancement in dynamic viscosity and consequently, a decline in velocity field is observed for greater values of viscosity parameter.

Figure (3.8) shows the effect of viscosity parameter on thermal distribution. The

relevant boundary layer shows declining fashion for increased values of viscosity parameter. Impact of Brownian diffusive motion and thermophoresis on thermal distribution is shown in Figures (3.9) and (3.10). The non predictive motion of nano particles due to the Brownian motion rises for stronger thermophoretic pressure, resulting in a greater rapid transport from hot region to the less warm region. Therefore, a upward push in thermal distribution is observed for both of the parameters. For multiplied values of viscosity parameter, we will see an enhancement in the concentration of distribution shown in Figure (3.11), which equally confirms the mathematical expression of viscosity parameter and its physical significance in fluid is proportional with the flow. For larger values of Brownian diffusive motion parameter, concentration profile shows reduction. Physically, the random motion reduces for large Brownian movement but, the case is opposite in case of thermophoresis. At $Nb = 0.01$, the impact of Brownian diffusion is pretty obvious but the effect becomes slighter for further increase in the Brownian diffusion, whereas a linear enhancement is seen in the attention distribution for $Nt = 0.01, 0.1, 0.2, 0.3$, in (3.13). The variation in Nusselt quantity is shown in Figures (3.14) and (3.15). In Figure (3.14), the impact of viscosity parameter and thermophoresis is shown, whereas in Figure (3.15), thermophoresis is changed with Brownian Diffusion. The rate of heat flux reduces in each case.

In Figure (3.16) and (3.17), the skin friction is plotted as function of viscosity parameter P by changing values of porosity and magnetic parameter respectively. The larger friction produced with the aid of Forchheimer medium and retardation presented by magnetic effects bring about enhancement of skin-friction. The impact of Prandtl range on thermal profile is proved in Figure (3.18). A decline is noticed for larger values of Pr .

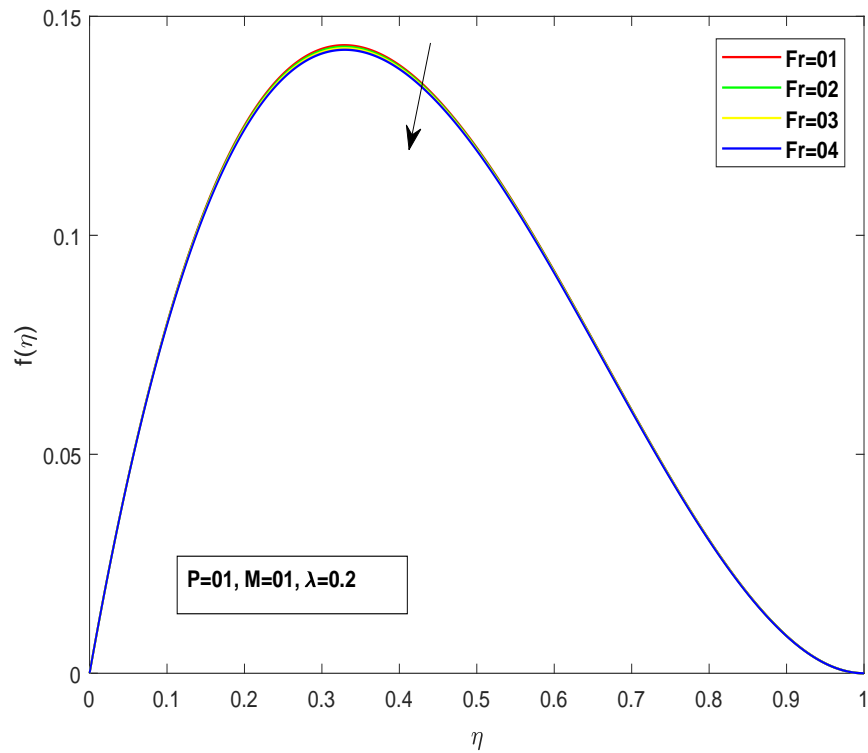


FIGURE 3.2: Consequences of Fr on $f(\eta)$.

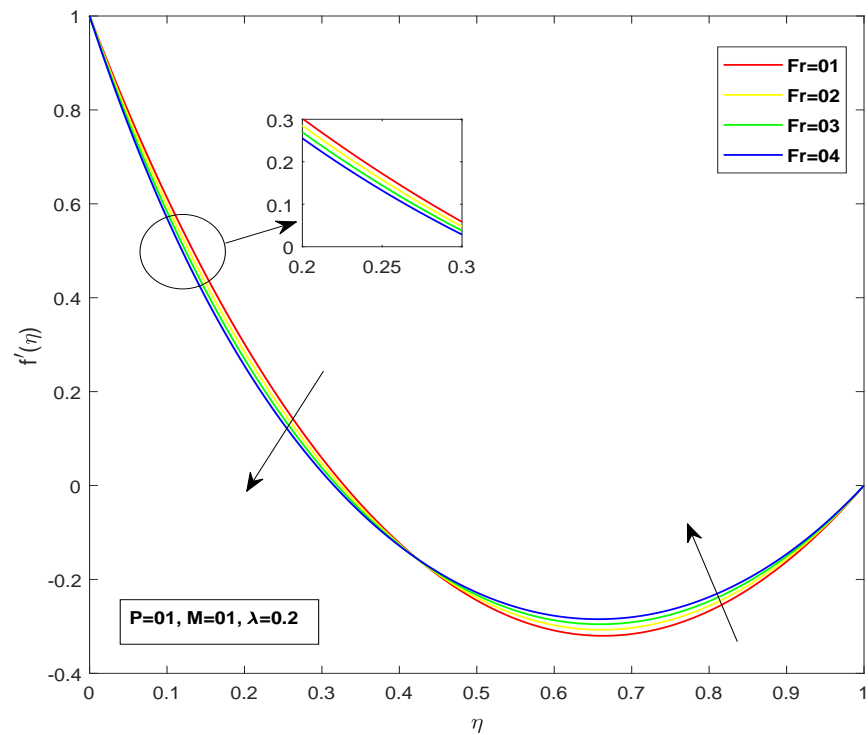


FIGURE 3.3: Consequences of Fr on $f'(\eta)$.

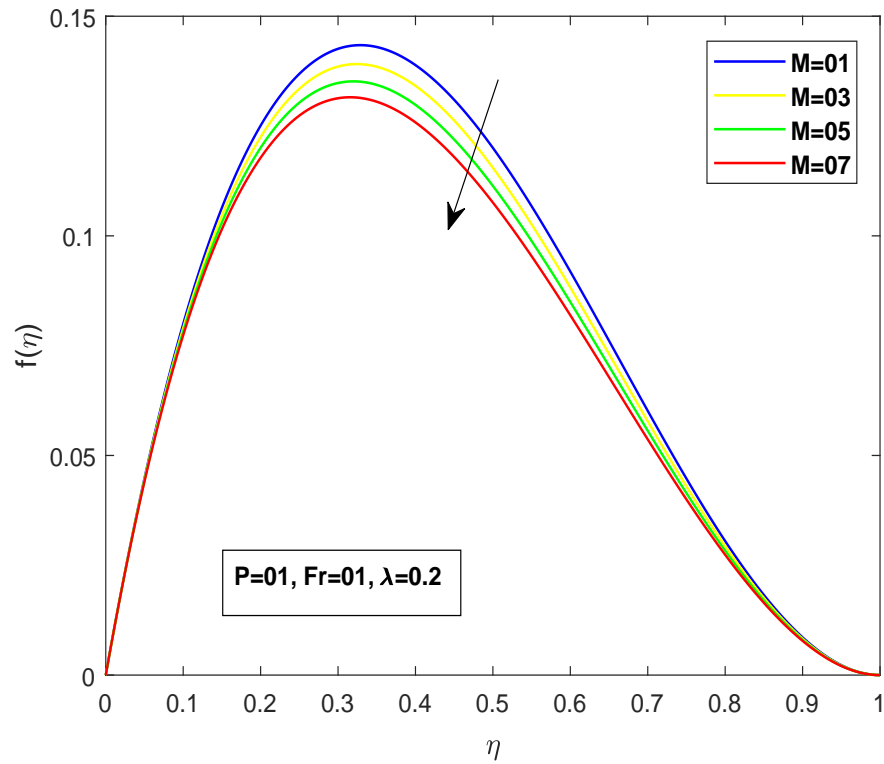


FIGURE 3.4: Consequences of M on $f(\eta)$.

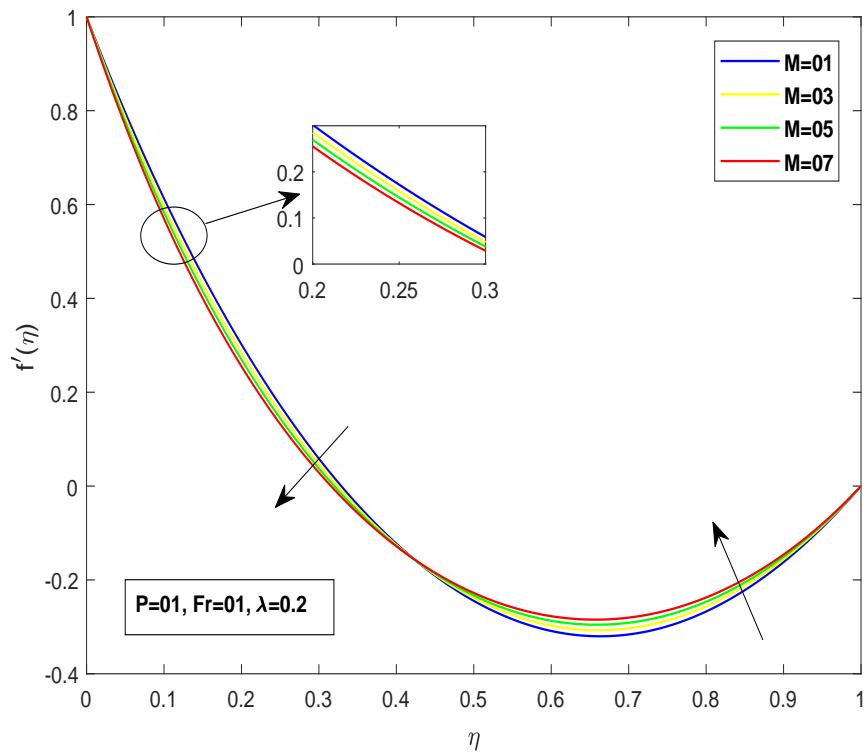
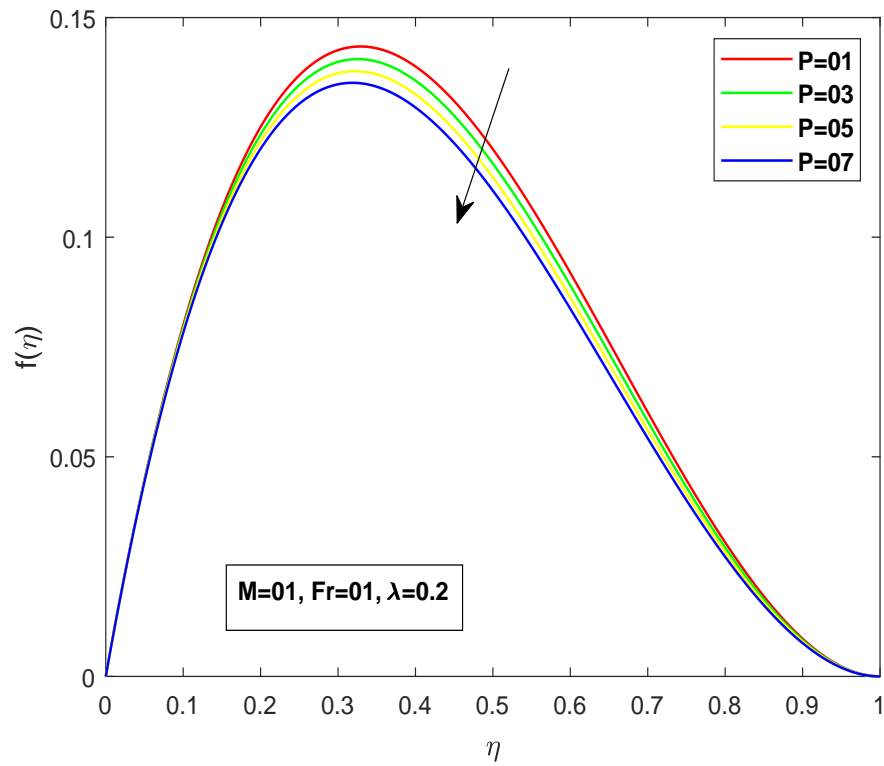
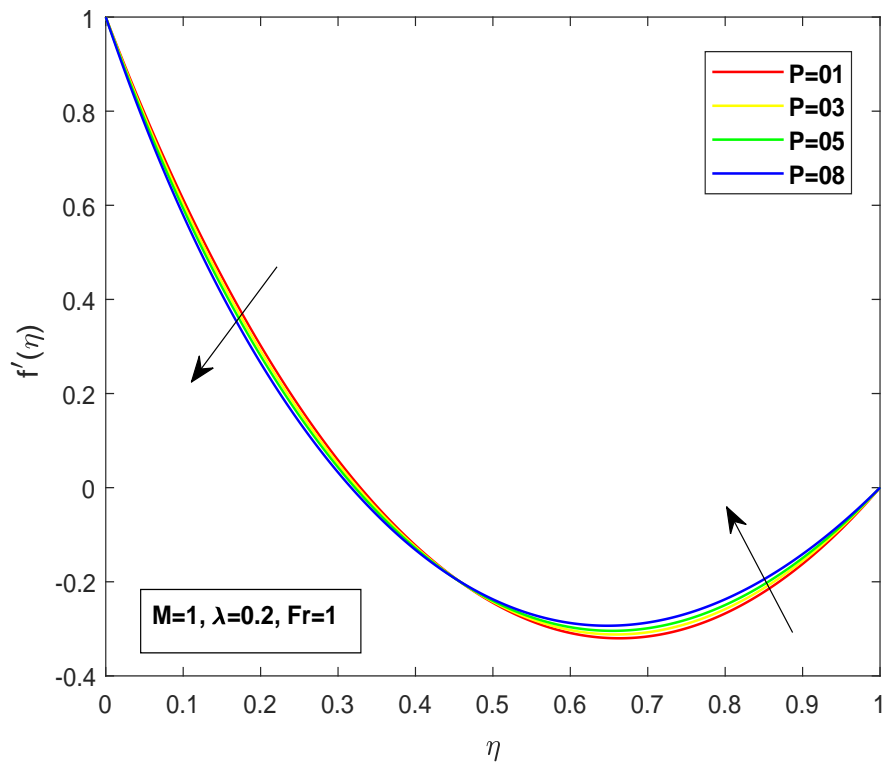


FIGURE 3.5: Consequences of M on $f'(\eta)$.

FIGURE 3.6: Consequences of P on $f(\eta)$.FIGURE 3.7: Consequences of P on $f'(\eta)$.

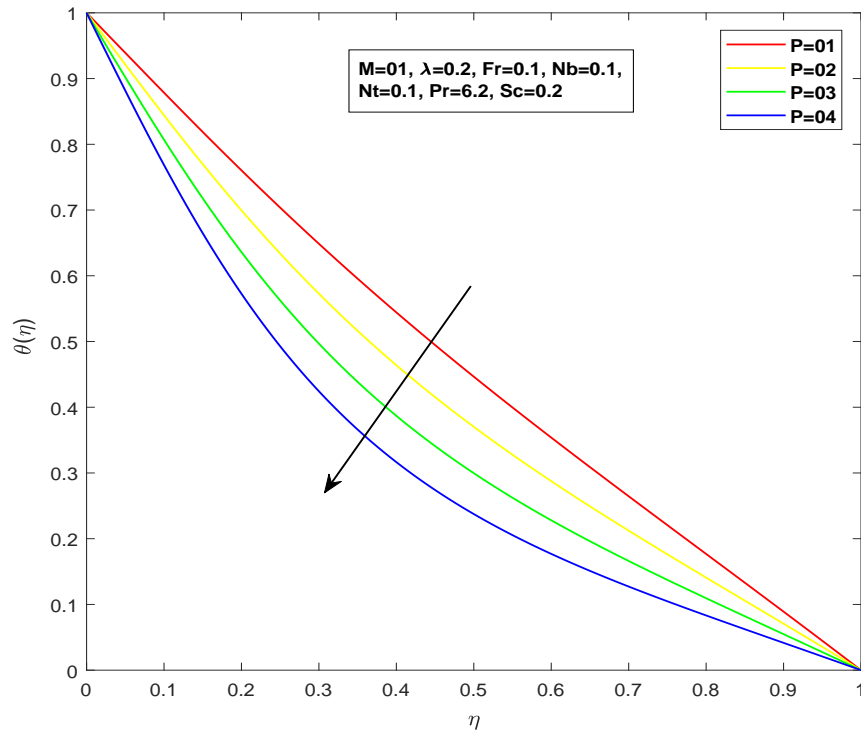


FIGURE 3.8: Consequences of P on $\theta(\eta)$.

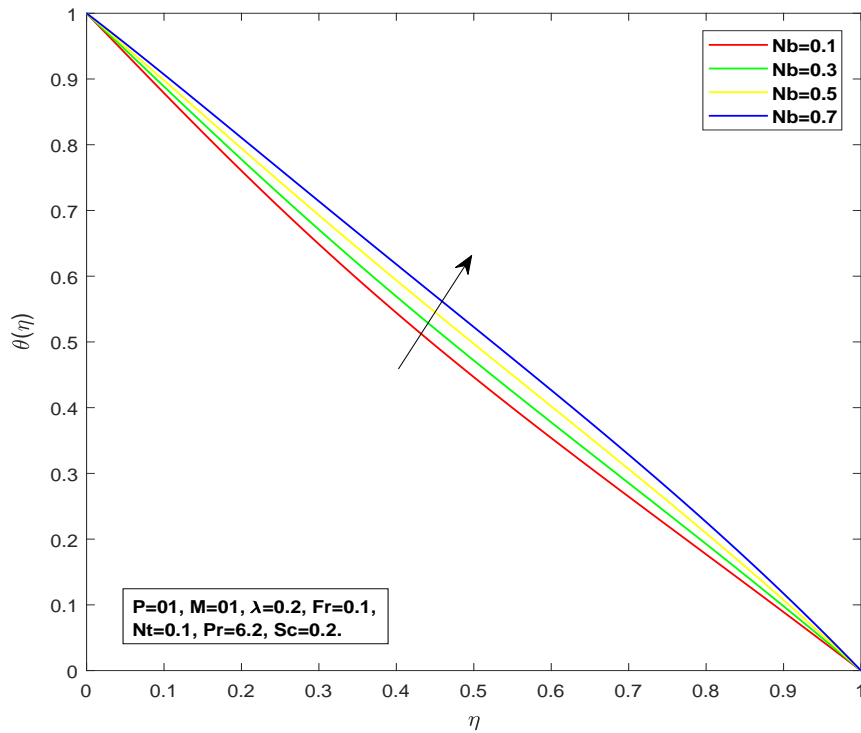
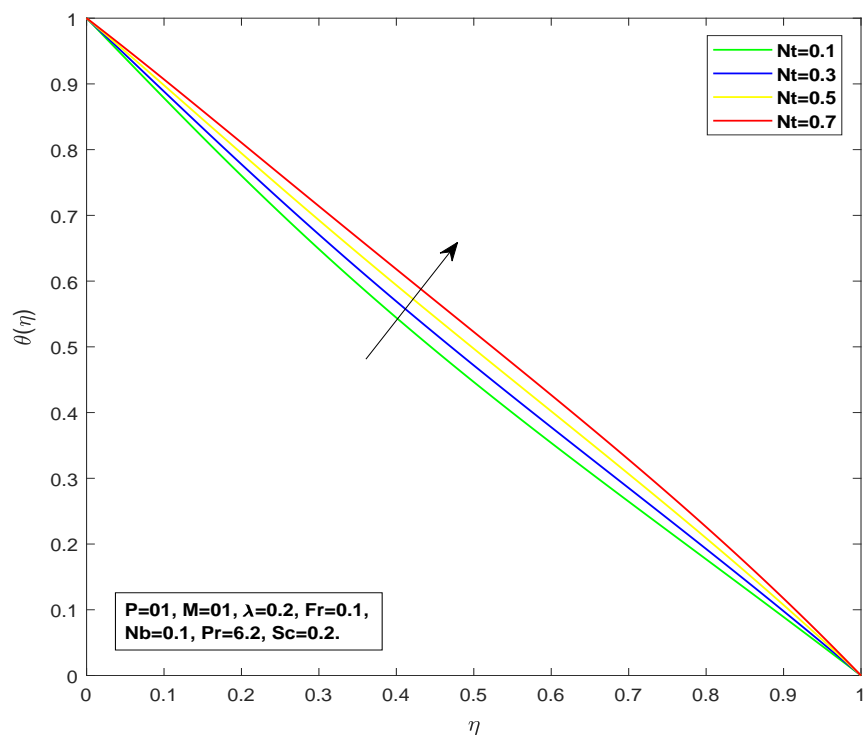
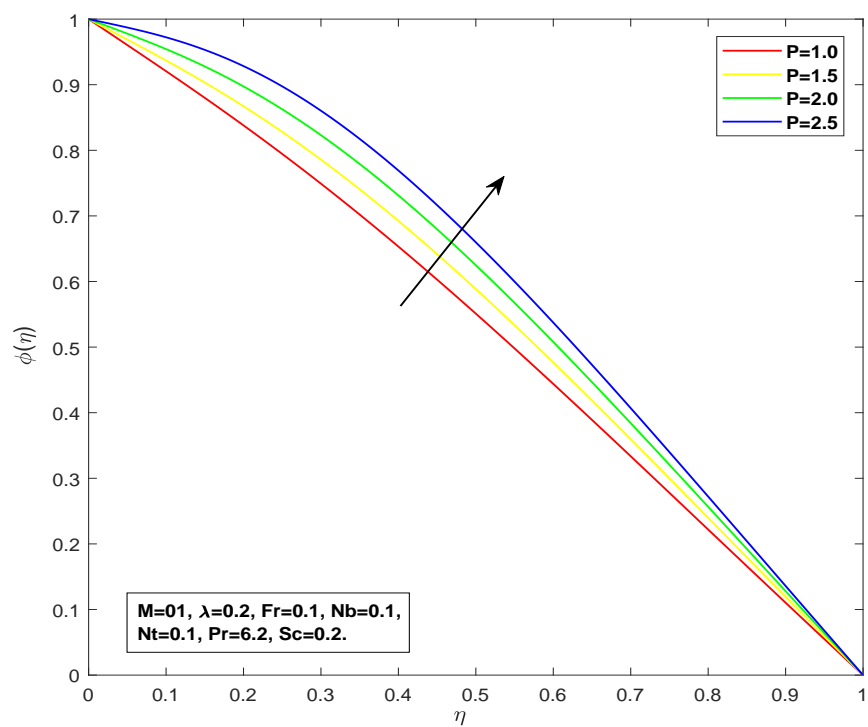


FIGURE 3.9: Consequences of Nb on $\theta(\eta)$.

FIGURE 3.10: Consequences of Nt on $\theta(\eta)$ FIGURE 3.11: Consequences of P on $\phi(\eta)$.

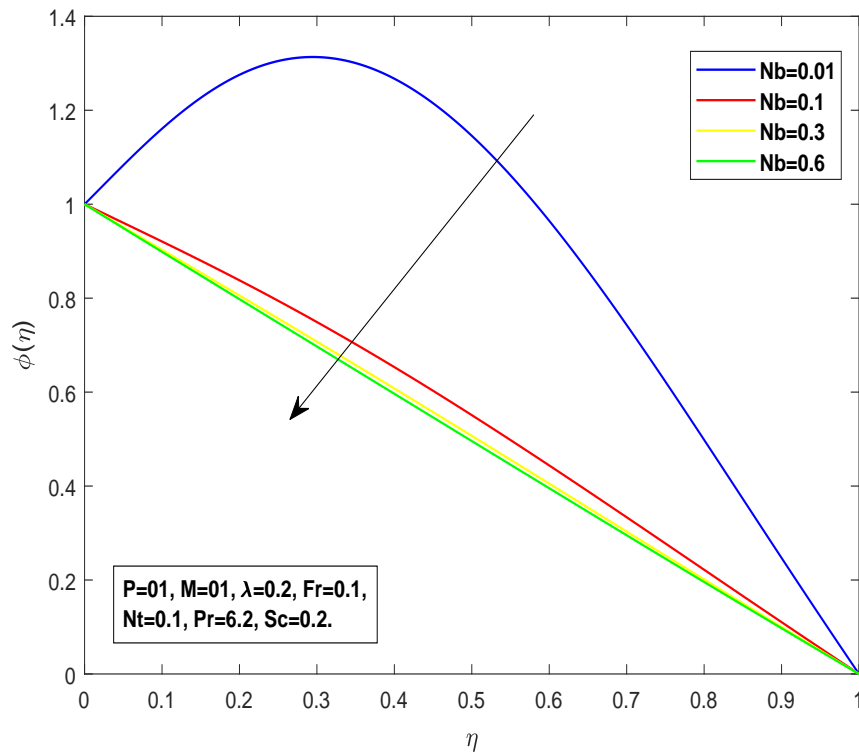


FIGURE 3.12: Consequences of Nb on $\phi(\eta)$.

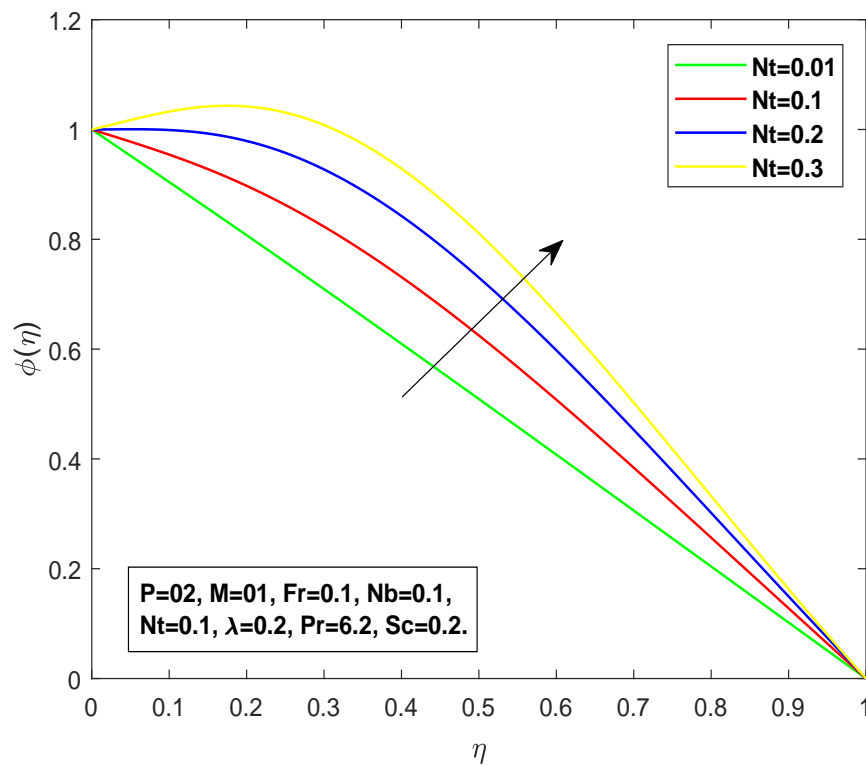


FIGURE 3.13: Consequences of Nt on $\phi(\eta)$.

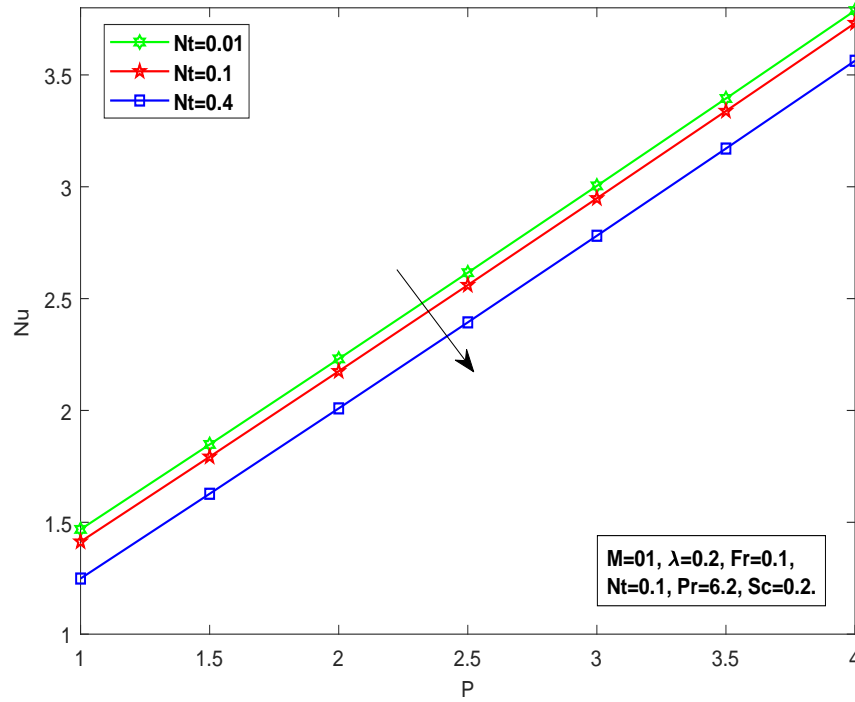


FIGURE 3.14: Variation in Nu for Viscosity Parameter P and Thermophoresis N_t .

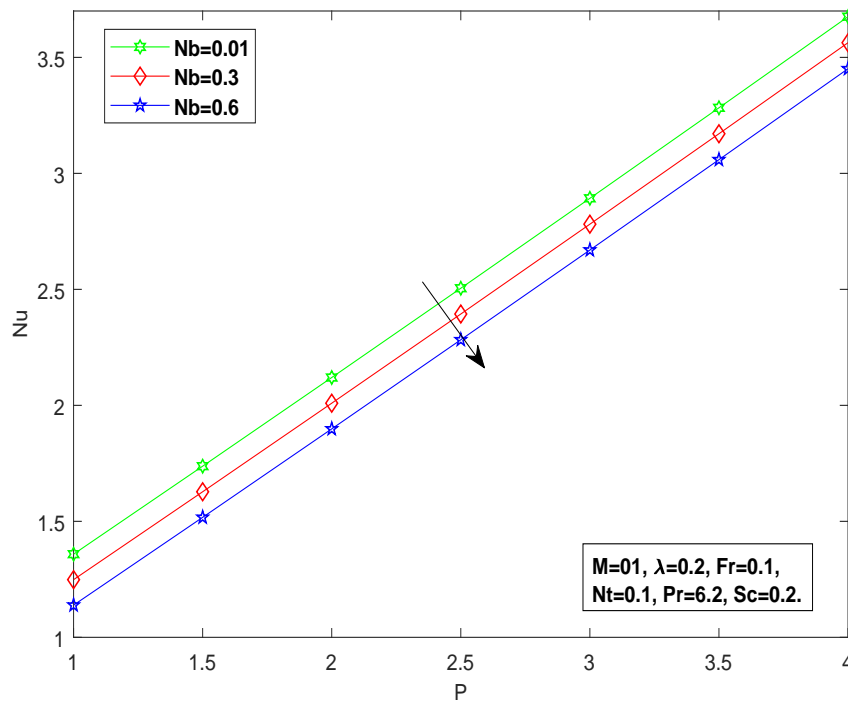


FIGURE 3.15: Variation in Nu for Viscosity Parameter P and Brownian Diffusion N_b .

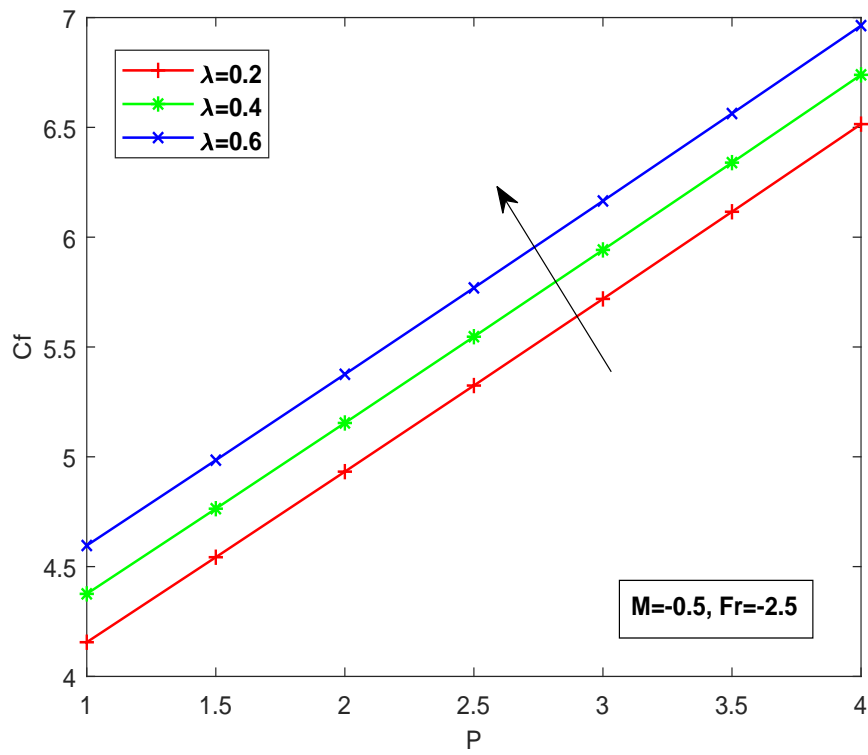


FIGURE 3.16: Variation in C_f for porosity factor λ .

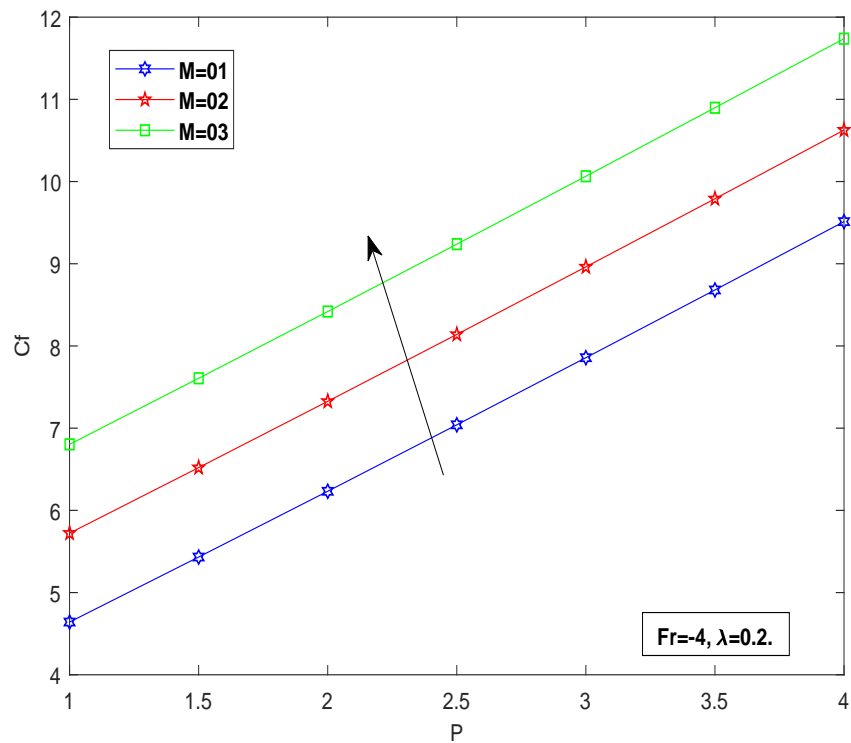
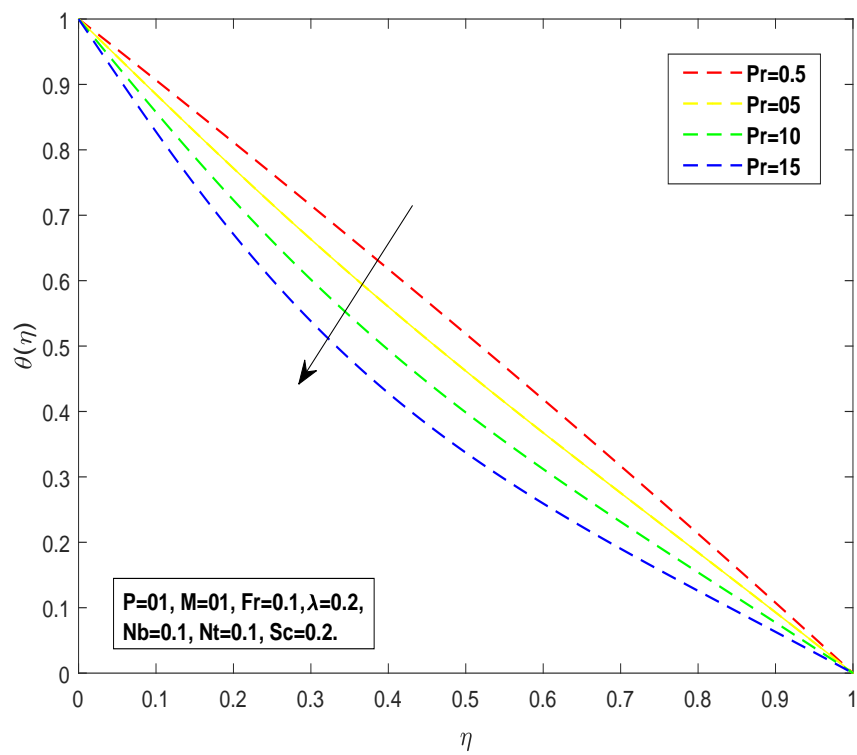


FIGURE 3.17: Variation in C_f for magnetic parameter M .

FIGURE 3.18: Consequences of P_r on $\theta(\eta)$.

Chapter 4

MHD Squeezed

Darcy-Forchheimer Casson Fluid

Flow between Horizontal Plates

4.1 Introduction

This chapter extends the work of Rasool et al.[1] by considering the inclined magnetic field, casson fluid, viscous dissipation and chemical reaction. The thermophoresis diffusion and Brownian motion are also included in the temperature equation. Furthermore concentration equation is also taken into account along with the chemical reaction. The governing nonlinear PDEs are converted into a system of dimensionless ODEs by utilizing the similarity transformations. The numerical solution of ODEs is obtained by applying numerical method known as shooting method. At the end of this chapter, the final results are discussed for significant parameters affecting $f'(\eta)$, $\theta(\eta)$ and $\phi(\eta)$ which are shown in graphs.

4.2 Mathematical Modeling

Consider a steady Casson fluid flow that is squeezed between two plates that are h distances apart and are adjusted horizontally. The location of plates is fixed at $x_2 = 0$ at one side and $x_2 = h$ at the other side in Cartesian coordinates. The bottom plate is stretched with at the rate of $u_1 = zx_1$, where z is a positive constant integer. A uniformly induced magnetic impact at an angle γ with the horizontal axis. Darcy-Forchheimer medium is considered between the plates, which allows the flow along horizontal axis with additional effects of porosity. Viscous dissipation is also taken into the account friction. [1]

Figure (4.1) showing inclined magnetic field.

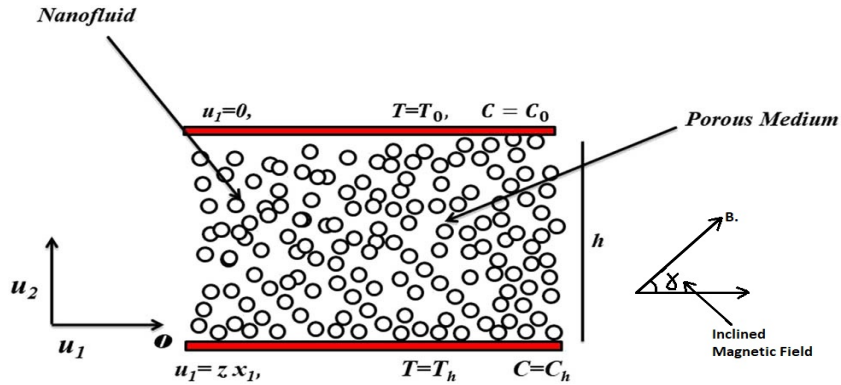


FIGURE 4.1: Geometry of the problem.

By considering the above assumptions, the governing PDEs are.

$$\frac{\partial u}{\partial x} + \frac{\partial v}{\partial y} = 0, \quad (4.1)$$

$$u_1 \frac{\partial u_1}{\partial x_1} + u_2 \frac{\partial u_1}{\partial x_2} = -\frac{1}{\rho_f} \frac{\partial p}{\partial x_1} + \nu \left(1 + \frac{1}{\beta}\right) \left(\frac{\partial^2 u_1}{\partial x_1^2} + \frac{\partial^2 u_1}{\partial x_2^2}\right) - \frac{\nu}{K} \left(1 + \frac{1}{\beta}\right) u_1 - F u_1^2 + \frac{\sigma B_0^2}{\rho_f} \sin \gamma (u_2 \cos \gamma - u_1 \sin \gamma), \quad (4.2)$$

$$u_1 \frac{\partial u_2}{\partial x_1} + u_2 \frac{\partial u_2}{\partial x_2} = -\frac{1}{\rho_f} \frac{\partial p}{\partial x_2} + \nu \left(1 + \frac{1}{\beta}\right) \left(\frac{\partial^2 u_2}{\partial x_1^2} + \frac{\partial^2 u_2}{\partial x_2^2}\right)$$

$$+ \frac{\sigma B_0^2}{\rho_f} \cos \gamma (u_1 \sin \gamma - u_2 \cos \gamma), \quad (4.3)$$

$$u_1 \frac{\partial T}{\partial x_1} + u_2 \frac{\partial T}{\partial x_2} = \alpha \left(\frac{\partial^2 T}{\partial x_1^2} + \frac{\partial^2 T}{\partial x_2^2} \right) + \tau \left[\left(D_B \left(\frac{\partial C}{\partial x_2} \frac{\partial T}{\partial x_2} + \frac{\partial C}{\partial x_1} \frac{\partial T}{\partial x_1} \right) + \frac{D_T}{T_h} \left(\frac{\partial T}{\partial x_1} \right)^2 + \left(\frac{\partial T}{\partial x_2} \right)^2 \right) \right] + \frac{\nu_f}{C_p} \left(\frac{\partial u_1}{\partial x_2} \right)^2, \quad (4.4)$$

$$u_1 \frac{\partial C}{\partial x_1} + u_2 \frac{\partial C}{\partial x_2} + K_c (C - C_h) = D_B \left(\frac{\partial^2 C}{\partial x_1^2} + \frac{\partial^2 C}{\partial x_2^2} \right) + \frac{D_T}{T_h} \left(\frac{\partial^2 T}{\partial x_1^2} + \frac{\partial^2 T}{\partial x_2^2} \right). \quad (4.5)$$

The associated BCs have been taken as.

$$\left. \begin{aligned} u_1 = u_w = zx_1, \quad u_2 = 0, \quad C = C_h, \quad T = T_h, \quad \text{at } x_2 = 0, \\ u_1 = 0, \quad C = C_0, \quad T = T_0, \quad \text{at } x_2 = +h. \end{aligned} \right\} \quad (4.6)$$

Following similarity transformation has been used to convert PDEs (4.1)-(4.5) into system of ODEs.

$$\left. \begin{aligned} u_1 &= zx_1 \frac{\partial f}{\partial \eta}, \\ u_2 &= -zhf, \\ \theta(\eta) &= \frac{T - T_h}{T_0 - T_h}, \\ \phi(\eta) &= \frac{C - C_h}{C_0 - C_h}. \end{aligned} \right\} \quad (4.7)$$

where f , θ , and ϕ are the dimensionless velocity, temperature and concentration of nanoparticles.

Continuity equation is satisfied which can be seen in chapter 3.

Differentiation of equations (4.2) w.r.t. x_2 and (4.3) w.r.t. x_1 and subtraction yield the following combined momentum equation:

$$\begin{aligned} & \frac{\partial u_1}{\partial x_1} \frac{\partial u_1}{\partial x_2} + u_1 \frac{\partial^2 u_1}{\partial x_1 \partial x_2} + \frac{\partial u_1}{\partial x_2} \frac{\partial u_2}{\partial x_2} + u_2 \frac{\partial^2 u_1}{\partial x_2^2} - \frac{\partial u_1}{\partial x_1} \frac{\partial u_2}{\partial x_1} - u_1 \frac{\partial^2 u_2}{\partial x_1^2} - \frac{\partial u_2}{\partial x_1} \frac{\partial u_2}{\partial x_2} \\ & - u_2 \frac{\partial^2 u_2}{\partial x_1 \partial x_2} = -\frac{1}{\rho_f} \frac{\partial^2 p}{\partial x_1 \partial x_2} + \nu \left(1 + \frac{1}{\beta} \right) \left(\frac{\partial^3 u_1}{\partial x_1^2 \partial x_2} + \frac{\partial^3 u_1}{\partial x_2^3} \right) \\ & + \frac{\sigma B_0^2}{\rho_f} \sin \gamma \left(\cos \gamma \frac{\partial u_2}{\partial x_2} - \sin \gamma \frac{\partial u_1}{\partial x_2} \right) - \frac{\nu}{K} \left(1 + \frac{1}{\beta} \right) \frac{\partial u_1}{\partial x_2} - 2Fu_1 \frac{\partial u_1}{\partial x_2} + \frac{1}{\rho_f} \frac{\partial^2 p}{\partial x_1 \partial x_2} \end{aligned}$$

$$\begin{aligned}
 & -\nu \left(1 + \frac{1}{\beta}\right) \left(\frac{\partial^3 u_2}{\partial x_2^2 \partial x_1} + \frac{\partial^3 u_2}{\partial x_1^3}\right) - \frac{\sigma B_0^2}{\rho_f} \cos \gamma \left(\sin \gamma \frac{\partial u_1}{\partial x_1} - \cos \gamma \frac{\partial u_2}{\partial x_1}\right), \\
 & \frac{\partial u_1}{\partial x_1} \frac{\partial u_1}{\partial x_2} + u_1 \frac{\partial^2 u_1}{\partial x_1 \partial x_2} + \frac{\partial u_1}{\partial x_2} \frac{\partial u_2}{\partial x_2} + u_2 \frac{\partial^2 u_1}{\partial x_2^2} - \frac{\partial u_1}{\partial x_1} \frac{\partial u_2}{\partial x_1} - u_1 \frac{\partial^2 u_2}{\partial x_1^2} - \frac{\partial u_2}{\partial x_1} \frac{\partial u_2}{\partial x_2} \\
 & - u_2 \frac{\partial^2 u_2}{\partial x_1 \partial x_2} = \nu \left(1 + \frac{1}{\beta}\right) \left(\frac{\partial^3 u_1}{\partial x_1^2 \partial x_2} + \frac{\partial^3 u_1}{\partial x_2^3} - \frac{\partial^3 u_2}{\partial x_2^2 \partial x_1} - \frac{\partial^3 u_2}{\partial x_1^3}\right) - \frac{\nu}{K} \left(1 + \frac{1}{\beta}\right) \frac{\partial u_1}{\partial x_2} \\
 & - 2F u_1 \frac{\partial u_1}{\partial x_2} + \frac{\sigma B_0^2}{\rho_f} \left(\sin \gamma \cos \gamma \frac{\partial u_2}{\partial x_2} - \sin^2 \gamma \frac{\partial u_1}{\partial x_2} - \sin \gamma \cos \gamma \frac{\partial u_1}{\partial x_1} + \cos^2 \gamma \frac{\partial u_2}{\partial x_1}\right).
 \end{aligned} \tag{4.8}$$

The complete procedure for the conversion of (4.2) and (4.3) discussed in Chapter 3.

$$\begin{aligned}
 & \left(1 + \frac{1}{\beta}\right) f^{iv} - P(f' f'' - f f''') - \lambda \left(1 + \frac{1}{\beta}\right) f'' \\
 & - 2F_r f' f'' - M \sin \gamma [\sin \gamma f'' - 2\delta \cos \gamma f'] = 0.
 \end{aligned}$$

Now, we include below the procedure for the conversion of equation (4.4) into the dimensionless form. The (4.10) and (4.11) we have already derived in chapter 3.

$$\begin{aligned}
 & u_1 \frac{\partial T}{\partial x_1} + u_2 \frac{\partial T}{\partial x_2} = \alpha \left(\frac{\partial^2 T}{\partial x_1^2} + \frac{\partial^2 T}{\partial x_2^2}\right) \\
 & + \tau \left[D_B \left(\frac{\partial C}{\partial x_2} \frac{\partial T}{\partial x_2} + \frac{\partial C}{\partial x_1} \frac{\partial T}{\partial x_1}\right) + \frac{D_T}{T_h} \left(\frac{\partial T}{\partial x_1}\right)^2 + \left(\frac{\partial T}{\partial x_2}\right)^2 + \frac{\nu_f}{C_P} \left(\frac{\partial u_1}{\partial x_2}\right)^2 \right], \\
 \Rightarrow & + z x_1 f'(0) + (-z h f) \frac{T_0 - T_h}{h} \theta' = \alpha \left(\frac{(T_0 - T_h)}{h^2} \theta''\right) \\
 & + \tau \left[D_B \left(\frac{(T_0 - T_h)}{h} \theta' \frac{C_0 - C_h}{h} \phi'\right) + \frac{D_T}{h} \left(\frac{(T_0 - T_h)^2}{h^2} \theta'^2\right) \right] + \frac{\nu_f}{C_P} \left(\frac{z x_1}{h} f''\right)^2, \\
 \Rightarrow & - z f(T_0 - T_h) \theta' = \alpha \frac{(T_0 - T_h)}{h^2} \theta'' \\
 & + \tau \left[D_B \frac{(T_0 - T_h)(C_0 - C_h)}{h^2} \theta' \phi' + \frac{D_T}{T_h} \frac{(T_0 - T_h)^2}{h^2} \theta'^2 \right] + \frac{\nu_f}{C_P} \left(\frac{z x_1}{h} f''\right)^2, \\
 \Rightarrow & - z f(T_0 - T_h) \theta' = \alpha \frac{(T_0 - T_h)}{h^2} \theta'' + \tau D_B \frac{(T_0 - T_h)(C_0 - C_h)}{h^2} \theta' \phi' \\
 & + \tau \frac{D_T}{T_h} \frac{(T_0 - T_h)^2}{h^2} \theta'^2 + \frac{\nu_f}{C_P} \frac{z^2 x_1^2}{h^2} f''^2,
 \end{aligned}$$

$$\begin{aligned}
 &\Rightarrow \alpha \frac{(T_0 - T_h)}{h^2} \theta'' + \tau D_B \frac{(T_0 - T_h)(C_0 - C_h)}{h^2} \theta' \phi' + z f (T_0 - T_h) \theta' \\
 &+ \tau \frac{D_T}{T_h} \frac{(T_0 - T_h)^2}{h^2} \theta'^2 + \frac{\nu_f}{C_P} \frac{z^2 x_1^2}{h^2} f''^2 = 0, \\
 &\Rightarrow \theta'' + \frac{h_2}{\alpha(T_0 - T_h)} \frac{\tau D_B (T_0 - T_h)(C_0 - C_h)}{h^2} \theta' \phi' + \frac{h_2}{\alpha(T_0 - T_h)} z f (T_0 - T_h) \theta' \\
 &+ \frac{h_2}{\alpha(T_0 - T_h)} \frac{\tau D_T}{T_h} \frac{(T_0 - T_h)^2}{h^2} \theta'^2 + \frac{\nu_f}{C_P \alpha} \frac{z^2 x_1^2}{(T_0 - T_h)} f''^2 = 0, \\
 &\Rightarrow \theta'' + \frac{\tau D_B (C_0 - C_h) h^2}{\alpha} \theta' \phi' + \frac{h^2 z f v}{\alpha v} \theta' + \frac{\tau D_T (T_0 - T_h)^2}{T_h \alpha} \theta'^2 \\
 &+ \frac{\nu_f}{C_P \alpha} \frac{z^2 x_1^2}{(T_0 - T_h)} f''^2 = 0, \\
 &N_t = \frac{\tau D_T (T_0 - T_h)}{\alpha T_h}, \quad N_b = \frac{\tau D_B (C_0 - C_h)}{\alpha}, \\
 &P = \frac{h^2 z}{v}, \quad P_r = \frac{v}{\alpha}, \\
 &\theta'' + N_b \theta' \phi' + \frac{h^2 z}{v} P_r f \theta' + N_t \theta'^2 + P_r E_c f''^2 = 0, \\
 &\theta'' + N_b \theta' \phi' + N_t \theta'^2 + P_r (P f \theta' + E_c f''^2) = 0.
 \end{aligned}$$

Now, we include below the procedure for the conversion of equation (4.5) into the dimensionless form.

$$\begin{aligned}
 &u_1 \frac{\partial C}{\partial x_1} + u_2 \frac{\partial C}{\partial x_2} + K_c (C_0 - C_h) = D_B \left(\frac{\partial^2 C}{\partial x_1^2} + \frac{\partial^2 C}{\partial x_2^2} \right) + \frac{D_T}{T_h} \left(\frac{\partial^2 T}{\partial x_1^2} + \frac{\partial^2 T}{\partial x_2^2} \right), \\
 &\Rightarrow u_1 \frac{\partial C}{\partial x_1} + u_2 \frac{\partial C}{\partial x_2} + K_c (C_0 - C_h) = D_B \left(\frac{\partial^2 C}{\partial x_1^2} + \frac{\partial^2 C}{\partial x_2^2} \right) + \frac{D_T}{T_h} \left(\frac{\partial^2 T}{\partial x_1^2} + \frac{\partial^2 T}{\partial x_2^2} \right), \\
 &\Rightarrow (-z h f) \frac{(C_0 - C_h)}{h} \phi' + K_c (C_0 - C_h) \phi = D_B \left(\frac{(C_0 - C_h)}{h^2} \phi'' \right) \\
 &+ \frac{D_T}{T_h} \left(\frac{(T_0 - T_h)}{h^2} \theta'' \right), \\
 &\Rightarrow -z f (C_0 - C_h) \phi' + K_c (C_0 - C_h) \phi = \frac{D_B (C_0 - C_h)}{h^2} \phi'' + \frac{D_T (T_0 - T_h)}{T_h h^2} \theta'', \\
 &\Rightarrow \frac{D_B (C_0 - C_h)}{h^2} \phi'' + z f (C_0 - C_h) \phi' + \frac{D_T (T_0 - T_h)}{T_h h^2} \theta'' - K_c (C_0 - C_h) \phi = 0, \\
 &\Rightarrow \phi'' + \frac{z h^2 f (C_0 - C_h)}{D_B (C_0 - C_h)} \phi' + \frac{D_T h^2}{T_h D_B (C_0 - C_h)} \frac{(T_0 - T_h)}{h^2} \theta'' - \frac{K_c (C_0 - C_h) h^2}{D_B (C_0 - C_h)} \phi = 0, \\
 &\Rightarrow \phi'' + \frac{z h_2 v}{v D_B} f \phi' + \frac{\tau D_T (T_0 - T_h)}{\alpha T_h} \frac{1}{\frac{\tau D_B (C_0 - C_h)}{\alpha}} \theta'' - \frac{K_c z h^2 v}{D_B v} \phi = 0, \\
 &\phi'' + P S_c f \phi' + \frac{N_t}{N_b} \theta'' - R S_c \phi = 0.
 \end{aligned}$$

The final dimensionless form of the governing model, is

$$\begin{aligned} & \left(1 + \frac{1}{\beta}\right) f^{iv} - P(f'f'' - ff''') - \lambda \left(1 + \frac{1}{\beta}\right) f'' \\ & - 2F_r f'f'' - M \sin \gamma [\sin \gamma f'' - 2\delta \cos \gamma f'] = 0, \end{aligned} \quad (4.9)$$

$$\theta'' + N_b \theta' \phi' + N_t \theta'^2 + P_r (Pf\theta' + E_c f''^2) = 0, \quad (4.10)$$

$$\phi'' + PS_c f \phi' + \frac{N_t}{N_b} \theta'' - RS_c \phi = 0. \quad (4.11)$$

The associated BCs (4.6) in the dimensionless form are,

$$\left. \begin{aligned} f = 0, \quad f' = 1, \quad \theta = 1 = \phi, \quad \text{at } \eta = 0, \\ f = 0, \quad f' = 0, \quad \theta = 0 = \phi, \quad \text{at } \eta = 1, \end{aligned} \right\} \quad (4.12)$$

Different parameters used in equations (4.9), (4.10) and (4.11) formulated as follows.

$$M = \frac{\sigma B_0^2 h^2}{\rho_f \nu}, \quad K_c = k_2 z, \quad R = \frac{k_2 z h^2}{\nu}, \quad \delta = \frac{h}{x_1}, \quad Pr = \frac{\nu}{\alpha},$$

$$Ec = \frac{z^2 x^2}{c_p (T_0 - T_h)}, \quad P = \frac{h^2 z}{\nu}, \quad S_c = \frac{\nu}{D_B}, \quad \lambda = \frac{h^2}{K},$$

$$F_r = \frac{F z h x_1}{\nu}, \quad Nb = \frac{\tau D_B (C_0 - C_h)}{\alpha}, \quad Nt = \frac{\tau D_T (T_0 - T_h)}{\alpha T_h}.$$

4.3 Numerical Treatment

This section is dedicated to the implementation of the shooting method to solve the transformed ODEs (4.9) (4.10) and (4.11) subject to the boundary conditions (4.6). One can easily observe that (4.9) independent of θ , so we will first find the solution of (4.9). For this purpose, the following notations are used:

$$\begin{aligned}
f &= y_1, \\
f' &= y_1' = y_2, \\
f'' &= y_2' = y_3, \\
f''' &= y_3' = y_4, \\
f^{iv} &= y_4'.
\end{aligned}$$

Utilizing the above notations, we have the following system of four first order differential equations.

$$\begin{aligned}
y_1' &= y_2; & y_1(0) &= 0, & y_1(1) &= 0, \\
y_2' &= y_3; & y_2(0) &= 1, & y_2(1) &= 0, \\
y_3' &= y_4; & y_3(0) &= R, \\
y_4' &= \left(\frac{\beta}{1+\beta}\right) P(y_2 y_3 - y_1 y_4) + \lambda y_3 - 2 \left(\frac{\beta}{1+\beta}\right) F_r y_2 y_3 \\
&+ M \left(\frac{\beta}{1+\beta}\right) \sin \gamma [\sin \gamma y_3 - 2\delta \cos \gamma y_2] = 0, & y_4(0) &= S.
\end{aligned}$$

To solve the above system by using Runge Kutta method of order four, two missing initial conditions are assumed to be R and S .

$$\begin{aligned}
y_1(\eta, R, S)_{\eta=1} - 0 &= 0, \\
y_2(\eta, R, S)_{\eta=1} - 0 &= 0.
\end{aligned}$$

Now

$$y_1(0) = y_2(0) = R, \quad y_3(0) = y_4(0) = S.$$

The Newton's method is used to solve algebraic equations system and has the following iterative scheme:

$$\begin{bmatrix} R^{n+1} \\ S^{n+1} \end{bmatrix} = \begin{bmatrix} R^n \\ S^n \end{bmatrix} - \begin{bmatrix} \frac{\partial y_1}{\partial R} & \frac{\partial y_1}{\partial S} \\ \frac{\partial y_2}{\partial R} & \frac{\partial y_2}{\partial S} \end{bmatrix}^{-1} \begin{bmatrix} y_1(1) - 0 \\ y_2(1) - 0 \end{bmatrix} \quad (4.13)$$

To incorporate the above formula, we further need the following derivatives:

$$\begin{aligned} \frac{\partial y_1}{\partial R} = y_5, \quad \frac{\partial y_2}{\partial R} = y_6, \quad \frac{\partial y_3}{\partial R} = y_7, \quad \frac{\partial y_4}{\partial R} = y_8, \\ \frac{\partial y_1}{\partial S} = y_9, \quad \frac{\partial y_2}{\partial S} = y_{10}, \quad \frac{\partial y_3}{\partial S} = y_{11}, \quad \frac{\partial y_4}{\partial S} = y_{12}. \end{aligned}$$

As the result of these notations, the Newton's iterative scheme gets the form:

$$\begin{bmatrix} R^{n+1} \\ S^{n+1} \end{bmatrix} = \begin{bmatrix} R^n \\ S^n \end{bmatrix} - \begin{bmatrix} y_5 & y_9 \\ y_6 & y_{10} \end{bmatrix}^{-1} \begin{bmatrix} y_1(1) - 0 \\ y_2(1) - 0 \end{bmatrix} \quad (4.14)$$

Now differentiate the above system of four first order ODE's (4.9) with respect to each of the variables R and S to have another system of eight ODE's together, the following IVP has:

$$\begin{aligned} y_1' &= y_2; & y_1(0) &= 0, \\ y_2' &= y_3; & y_2(0) &= 0, \\ y_3' &= y_4; & y_3(0) &= R, \\ y_4' &= \left(\frac{\beta}{1+\beta}\right) P(y_2 y_3 - y_1 y_4) + \lambda y_3 - 2 \left(\frac{\beta}{1+\beta}\right) F_r y_2 y_3 \\ &+ M \left(\frac{\beta}{1+\beta}\right) \sin \gamma [\sin \gamma y_3 - 2\delta \cos \gamma y_2] = 0; & y_4(0) &= S, \\ y_5' &= y_6; & y_5(0) &= 0, \\ y_6' &= y_7; & y_6(0) &= 0, \\ y_7' &= y_8; & y_7(0) &= 1, \\ y_8' &= \left(\frac{\beta}{1+\beta}\right) P(y_3 y_6 + y_2 y_7 - y_4 y_5 - y_1 y_8) + \lambda y_7 - 2 \left(\frac{\beta}{1+\beta}\right) F_r (y_3 y_6 + y_2 y_7) \\ &+ M \left(\frac{\beta}{1+\beta}\right) \sin \gamma [\sin \gamma y_7 - 2\delta \cos \gamma y_6] = 0; & y_8(0) &= 0, \\ y_9' &= y_{10}; & y_9(0) &= 0, \end{aligned}$$

$$\begin{aligned}
y'_{10} &= y_{11}; & y_{10}(0) &= 0, \\
y'_{11} &= y_{12}; & y_{11}(0) &= 0, \\
y'_{12} &= \left(\frac{\beta}{1+\beta} \right) P(y_3 y_{10} + y_2 y_{11} - y_4 y_9 - y_1 y_{12}) + \lambda y_{11} - 2 \left(\frac{\beta}{1+\beta} \right), \\
F_r(y_3 y_{10} + y_2 y_{11}) + M \left(\frac{\beta}{1+\beta} \right) \sin \gamma [\sin \gamma y_{11} - 2\delta \cos \gamma y_{10}] &= 0; & y_{12}(0) &= 1,
\end{aligned}$$

The Runge Kutta method of order four is used to solve the above system of twelve first order differential equations with R and S as initial guess. The iterative process is repeated until the criteria listed below are met:

$$\max [|y_1(\eta, R, S)|, |y_2(\eta, R, S)|] < \epsilon$$

for an arbitrarily small positive value of ϵ . Throughout this chapter ϵ has been taken as $(10)^{-6}$. Since (4.10) and (4.11) are coupled equations. So (4.10) will be solved separately by incorporating the solution of (4.11). For this purpose let us denote:

$$\theta = Y_1, \quad \theta' = Y_1' = Y_2, \quad \theta'' = Y_2',$$

and

$$\phi = Y_3, \quad \phi' = Y_3' = Y_4, \quad \phi'' = Y_4' = Y_5,$$

and

$$f = D, \quad f'' = G.$$

to get the following first order ODE's.

$$\begin{aligned}
Y_1' &= Y_2; & Y_1(0) &= 1, & Y_1(1) &= 0, \\
Y_2' &= -N_b Y_4 Y_2 + N_t Y_2^2 - P_r (P D Y_2 + E_c G^2); & Y_2(0) &= R, \\
Y_3' &= Y_4; & Y_3(0) &= 1, & Y_3(1) &= 0, \\
Y_4' &= -P S_c D Y_4 - \frac{N_t}{N_b} Y_3 + R S_c Y_3; & Y_4(0) &= S.
\end{aligned}$$

The above IVP is solved numerically by Runge Kutta method of order four. In the above initial value problem, the missing condition m is to be chosen such that:

$$\begin{aligned} Y_1(\eta, R, S)_{\eta=1} - 0 &= 0, \\ Y_3(\eta, R, S)_{\eta=1} - 0 &= 0. \end{aligned}$$

Now

$$Y_1(0) = Y(0) = R, \quad Y_2(0) = Y'(0) = S.$$

The Newton's method is used to solve algebraic equations system and has the following iterative scheme:

$$\begin{bmatrix} R^{n+1} \\ S^{n+1} \end{bmatrix} = \begin{bmatrix} R^n \\ S^n \end{bmatrix} - \begin{bmatrix} \frac{\partial Y_1}{\partial R} & \frac{\partial Y_1}{\partial S} \\ \frac{\partial Y_3}{\partial R} & \frac{\partial Y_3}{\partial S} \end{bmatrix}^{-1} \begin{bmatrix} Y_1(1) - 0 \\ Y_3(1) - 0 \end{bmatrix} \quad (4.15)$$

To incorporate the above formula, we further need the following derivatives:

$$\begin{aligned} \frac{\partial Y_1}{\partial R} &= Y_5, & \frac{\partial Y_2}{\partial R} &= Y_6, \\ \frac{\partial Y_3}{\partial R} &= Y_7, & \frac{\partial Y_4}{\partial R} &= Y_8, \\ \frac{\partial Y_1}{\partial S} &= Y_9, & \frac{\partial Y_2}{\partial S} &= Y_{10}, \\ \frac{\partial Y_3}{\partial S} &= Y_{11}, & \frac{\partial Y_4}{\partial S} &= Y_{12}. \end{aligned}$$

As the result of these notations, the Newton's iterative scheme gets the form:

$$\begin{bmatrix} R^{n+1} \\ S^{n+1} \end{bmatrix} = \begin{bmatrix} R^n \\ S^n \end{bmatrix} - \begin{bmatrix} Y_5 & Y_9 \\ Y_7 & Y_{11} \end{bmatrix}^{-1} \begin{bmatrix} Y_1(1) - 0 \\ Y_3(1) - 0 \end{bmatrix} \quad (4.16)$$

Here n is the number of iterations ($n = 0, 1, 2, 3, 4, 5, \dots$).

Now differentiate the above system of four first order ODE's (4.15) with respect to each of the variables R and S to have another system of eight ODE's together,

the following IVP has:

$$\begin{aligned}
Y_1' &= Y_2; & Y_1(0) &= 1, \\
Y_2' &= -N_b Y_4 Y_2 + N_t Y_2^2 - P_r (P D Y_2 + E_c G^2); & Y_2(0) &= R, \\
Y_3' &= Y_4; & Y_3(0) &= 1, \\
Y_4' &= -P S_c D Y_4 - \frac{N_t}{N_b} Y_3 + R S_c Y_3; & Y_4(0) &= S, \\
Y_5' &= Y_6; & Y_5(0) &= 0, \\
Y_6' &= -N_b (Y_2 Y_8 + Y_4 Y_6) + 2 N_t Y_2 Y_6 - P_r P D Y_6; & Y_6(0) &= 1, \\
Y_7' &= Y_8; & Y_7(0) &= 0, \\
Y_8' &= -P S_c D Y_8 - \frac{N_t}{N_b} Y_7 + R S_c Y_7; & Y_8(0) &= 0, \\
Y_9' &= Y_{10}; & Y_9(0) &= 0, \\
Y_{10}' &= -N_b (Y_2 Y_{12} + Y_4 Y_{10}) + 2 N_t Y_2 Y_{10} - P_r P D Y_{10}; & Y_{10}(0) &= 0, \\
Y_{11}' &= Y_{12}; & Y_{11}(0) &= 0, \\
Y_{12}' &= -P S_c D Y_{12} - \frac{N_t}{N_b} Y_{11} + R S_c Y_{11}; & Y_{12}(0) &= 1.
\end{aligned}$$

The Runge Kutta method of order four is used to solve the above system of twelve first order differential equations with R and S initial guess. The iterative process is repeated until the criteria listed below are met:

$$\max [| Y_1(\eta, R, S) |, | Y_3(\eta, R, S) |] < \epsilon$$

for an arbitrarily small positive value of ϵ . Throughout this chapter ϵ was taken as $(10)^{-6}$.

4.4 Representation of Graphs

This section explores the graphical outcomes and their physical justifications for the three essential profiles such as speed, temperature and nanoparticle concentration. Figures 4.2 to 4.18 are plotted to expose the consequences of several fluid parameters disconcerted in the present flow model.

Figures (4.2) and (4.3) are the graphical descriptions of the effect of the Forchheimer parameter on velocity f and f' respectively. A nearer appearance elaborates that the velocity region decreases with increase in the Forchheimer number. Physically, the relation of Forchheimer amount with drag force coefficient is responsible for this fashion in velocity parameter. For more Forchheimer variety an exhaustive range is available, and drag stress coefficient results in a larger amount of friction supplied to the fluid flow. Therefore, a decline is observed in respect of the velocity profile.

Figures (4.4) and (4.5) indicate the impact of magnetic field on fluid flow through Darcy Medium. The impact of magnetic area is inversely associated with the flow of stated fluid. A surface normal implementation of magnetic region creates positive bumps in the direction, of fluid flow therefore, a decline is determined in each f and f' . Figures (4.6) and (4.7) reveals the impact of viscosity parameter P on both f and f' respectively. Physically, for bigger values of P , the inverse relation of kinematic viscosity confirms the enhancement in dynamic viscosity, and consequently, a decline in velocity field is observed for more values of viscosity parameter.

Figure (4.8) suggests the impact of viscosity parameter on thermal distribution. The applicable boundary layer indicates declining style for increased values of viscosity parameter. Impact of Brownian diffusive movement and thermoplastics on thermal distribution is shown in Figures (4.9) and (4.10). The non-predictive movement of nanoparticles because of the Brownian movement rises for stronger thermoplastic pressure, ensuing in a greater fast delivery from warm vicinity to the less heat place. Therefore, an upward thrust in thermal distribution is discovered for each the parameters. For multiplied values of viscosity parameter, we may

see an enhancement in the concentration of distribution proven in Figure (4.11), which equally confirms the mathematical expression of viscosity parameter and its physical significance in fluid is proportional to the flow. For progressed values of Brownian diffusive movement parameter, concentration profile exhibits reduction. Physically, the random movement reduces for enhanced Brownian motion but, the case is contrary in case of thermophoresis. At $Nb = 0.01$, the effect of Brownian diffusion is quite obvious however the impact will slightly reduced. In addition improvement in the Brownian diffusion, while a linear enhancement is visible in the attention distribution for Nt . Figure (4.14) and Figure (4.15) are plotted by taking Nu as function of viscosity parameter P for different values of thermophoresis Nt and Brownian Diffusion parameter Nb . It can be seen in Figure (4.14) that with increase in P . Nu is increasing and for a fixed value of P by increasing Nt , a decline in Nu can be seen. Same behaviour can be seen in Figure (4.15) for values of Nb .

Figures (4.16) and (4.17) are plotted to estimate the fluctuation in skin-friction as a function of viscosity parameter, by change the values of λ and M respectively. The larger friction produced with the useful resource of Forchheimer medium and retardation provided through magnetic effect results in the enhancement of skin-friction. The effect of Prandtl number on thermal profile is demonstrated in Figure (4.18), that shows a decline in temperature profile for large values of Pr .

In Figure (4.19) we plotted skin-friction as a function an angle of inclination γ by changing vales of porosity factor λ . we can see decrease in C_f by increasing value of λ .

In Figure (4.20) we plotted Nusselt number as function an angle of inclination γ by changing values of porosity factor λ . We can see decrease in Nusselt number by increasing value of λ .

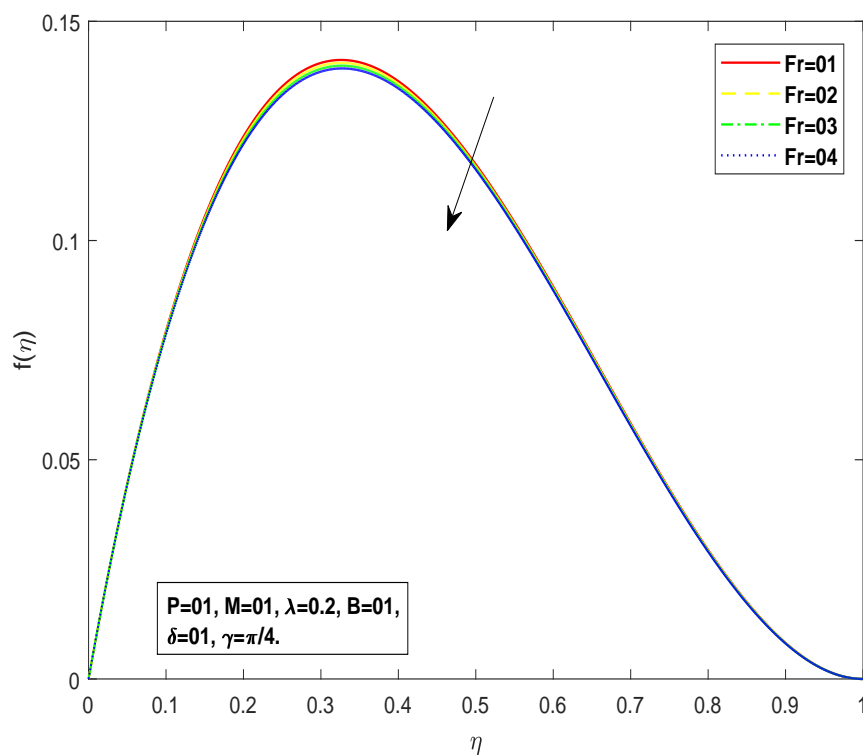


FIGURE 4.2: Consequences of F_r on $f(\eta)$.

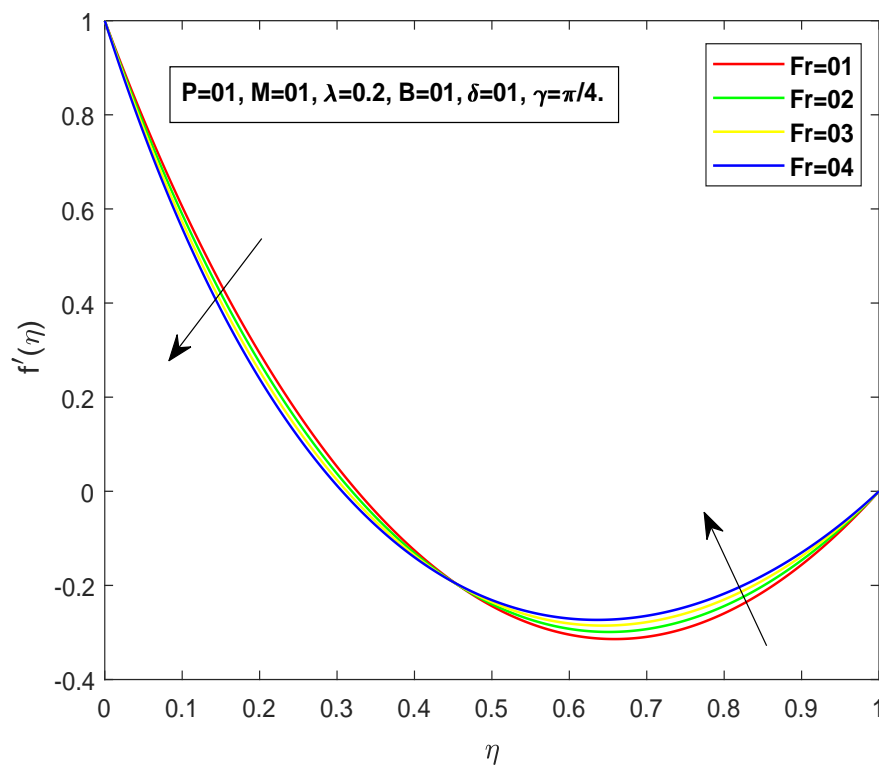


FIGURE 4.3: Consequences of F_r on $f'(\eta)$.

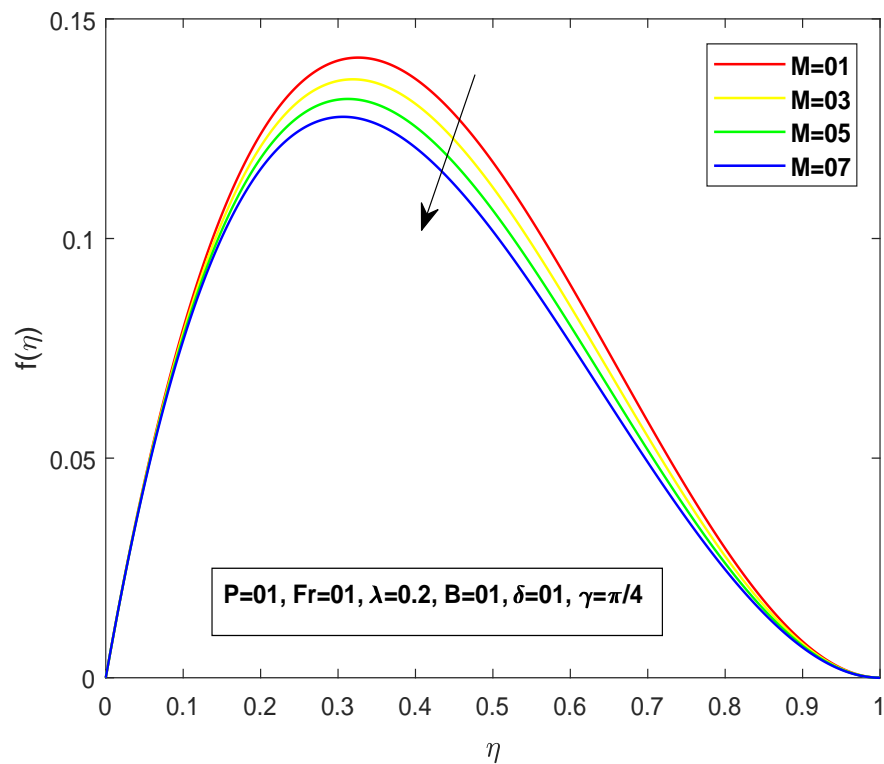


FIGURE 4.4: Consequences of M on $f(\eta)$.

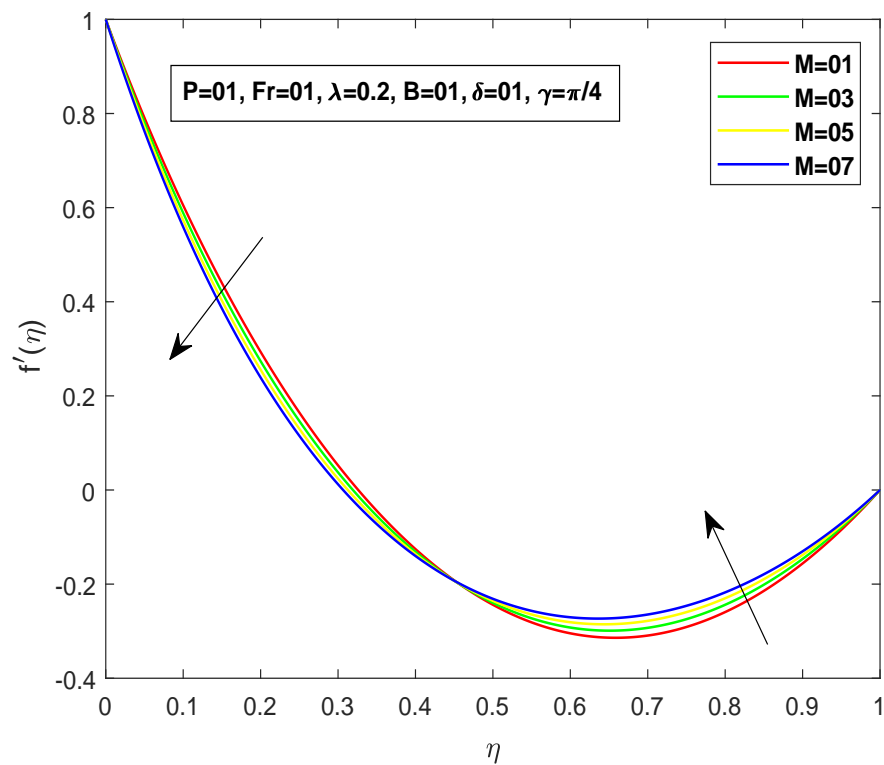


FIGURE 4.5: Consequences of M on $f'(\eta)$.

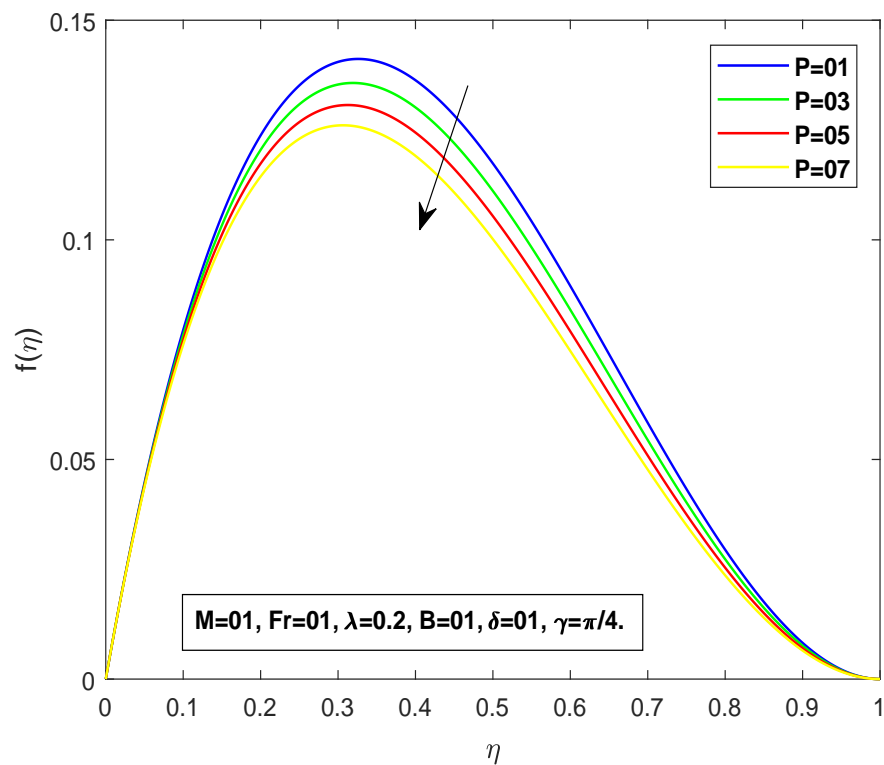


FIGURE 4.6: Consequences of P on $f(\eta)$.

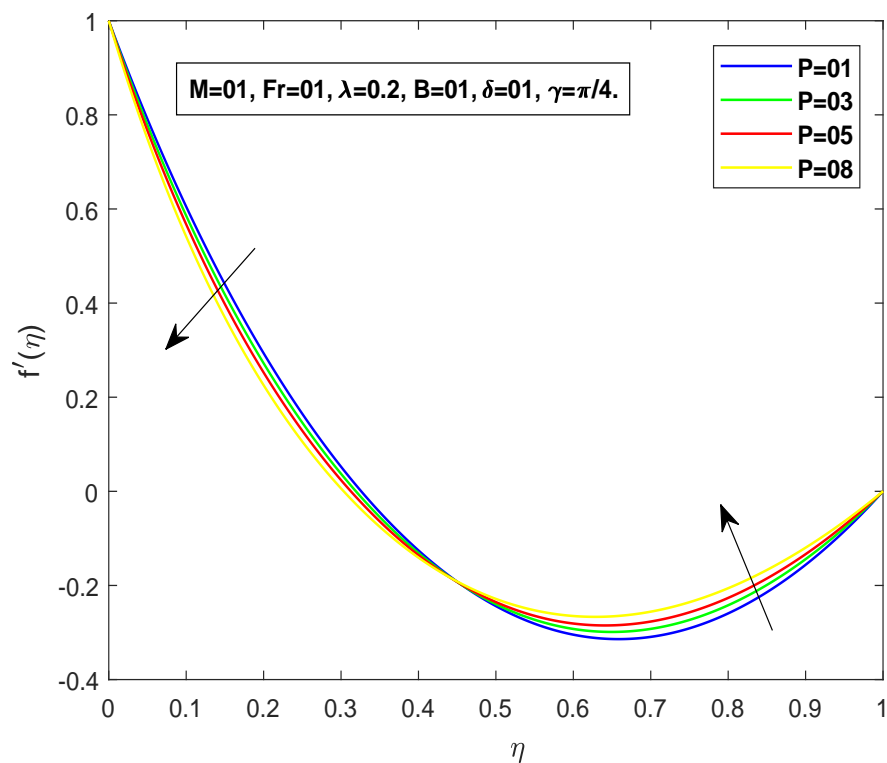


FIGURE 4.7: Consequences of P on $f'(\eta)$.

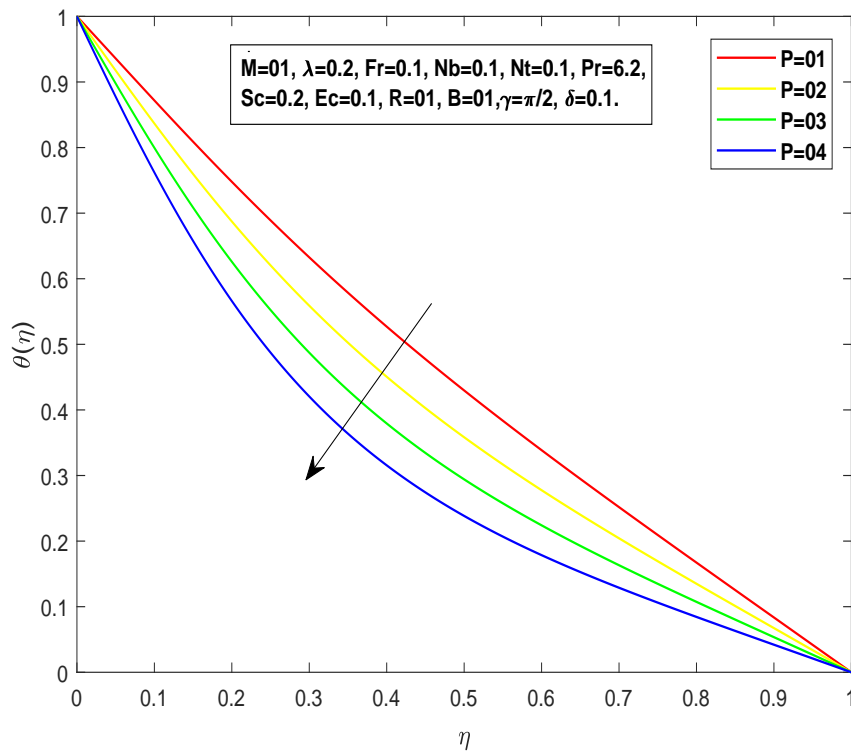


FIGURE 4.8: Consequences of P on $\theta(\eta)$.

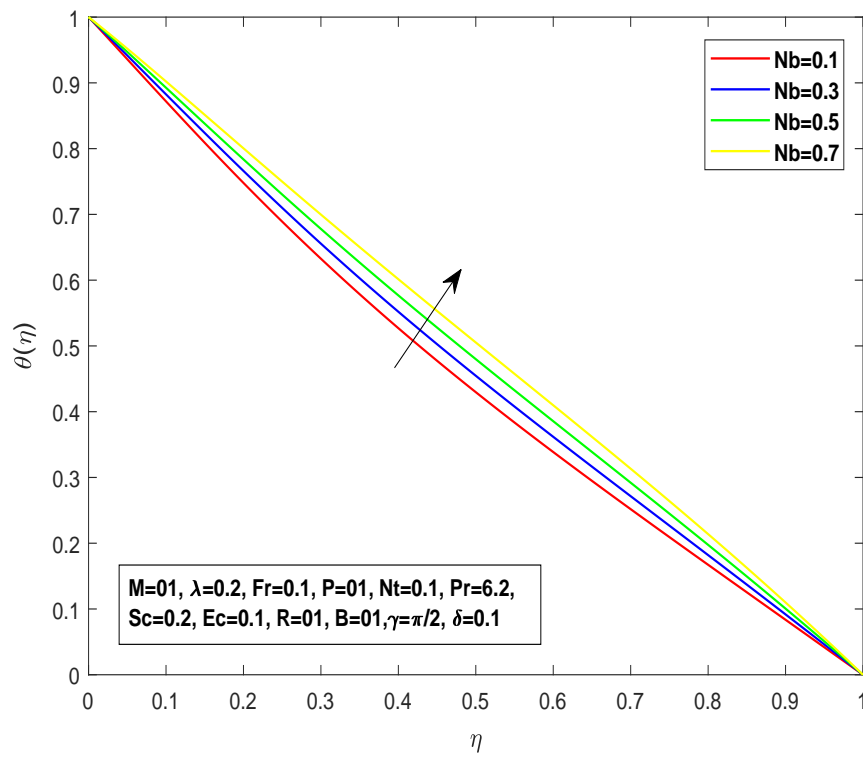


FIGURE 4.9: Consequences of Nb on $\theta(\eta)$.

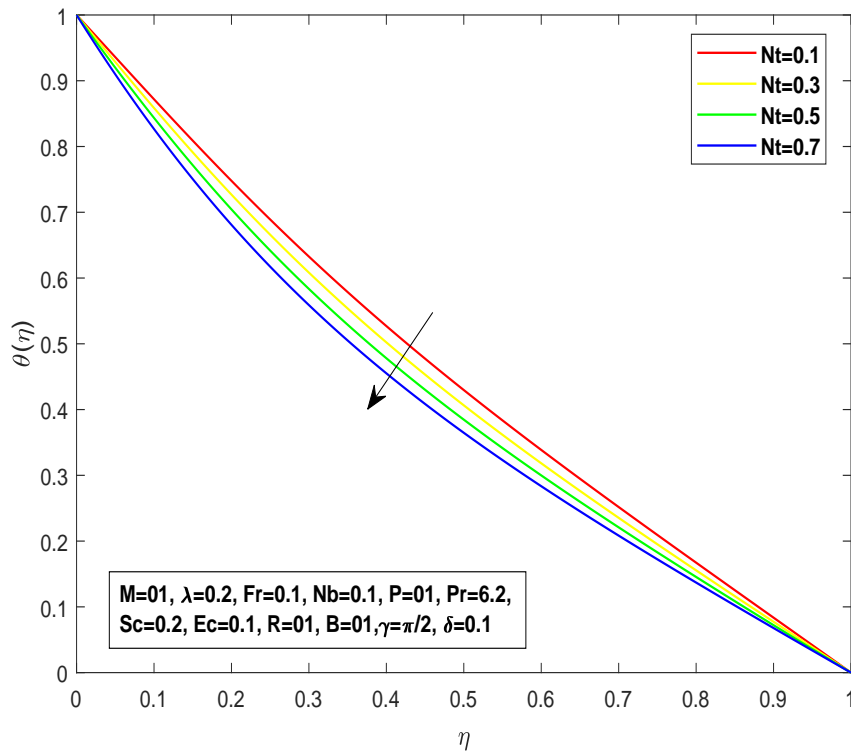


FIGURE 4.10: Consequences of Nt on $\theta(\eta)$.

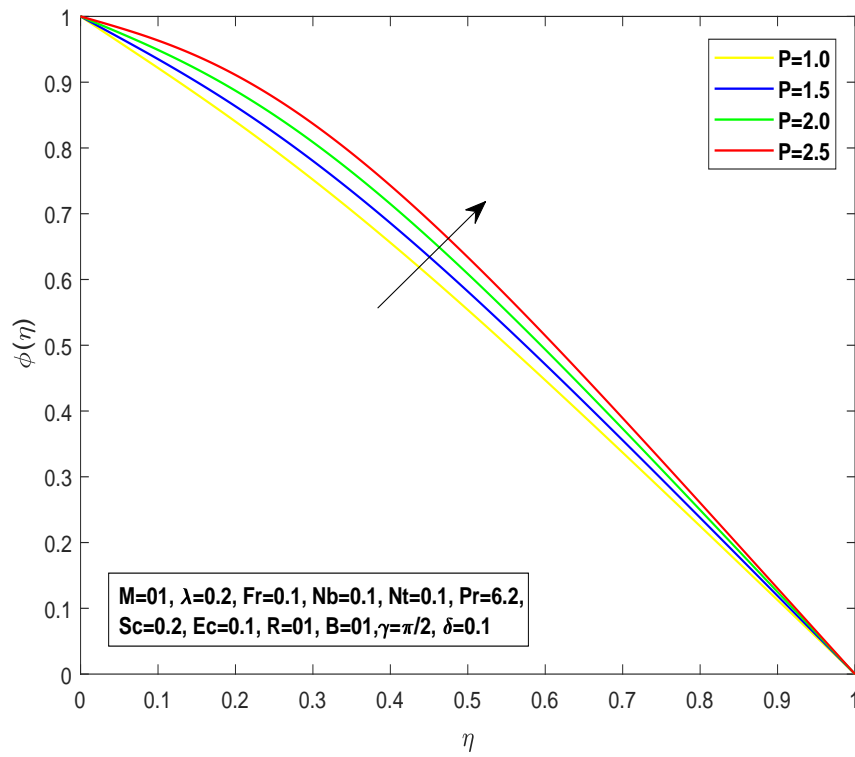


FIGURE 4.11: Consequences of P on $\phi(\eta)$.

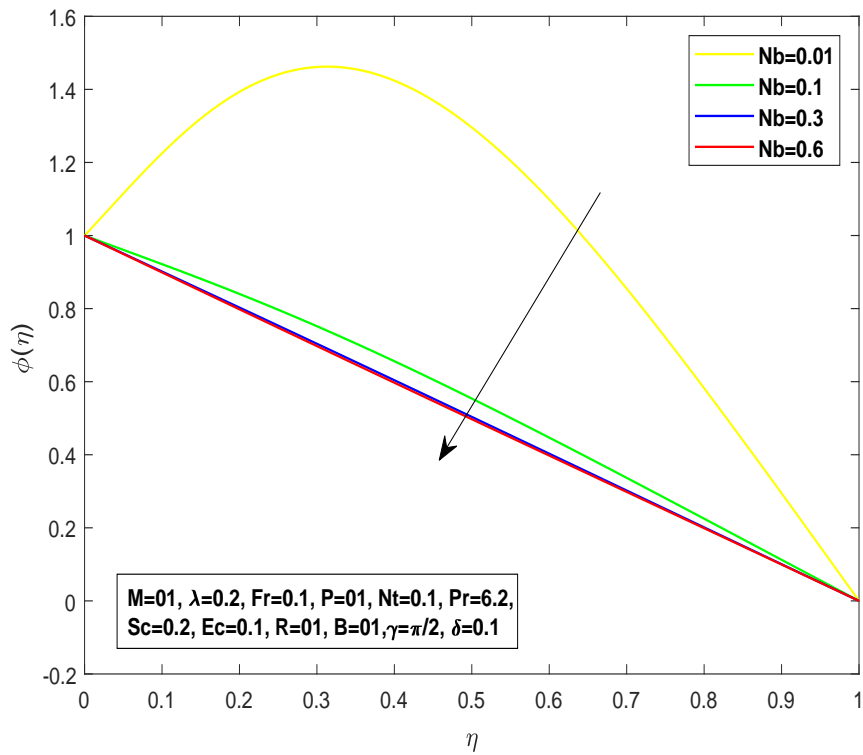


FIGURE 4.12: Consequences of Nb on $\phi(\eta)$.

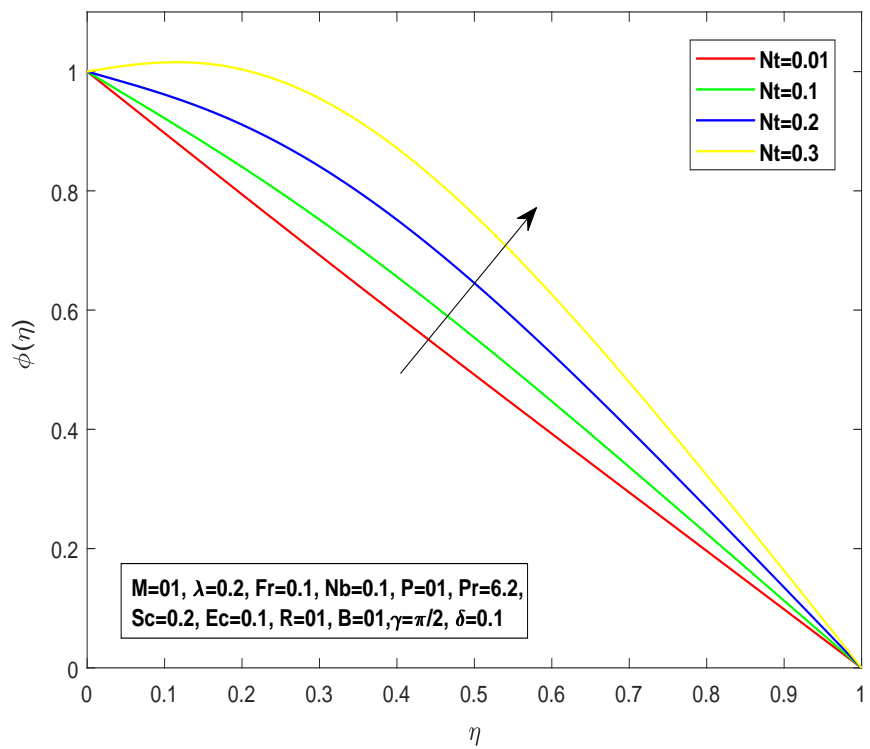


FIGURE 4.13: Consequences of Nt on $\phi(\eta)$.

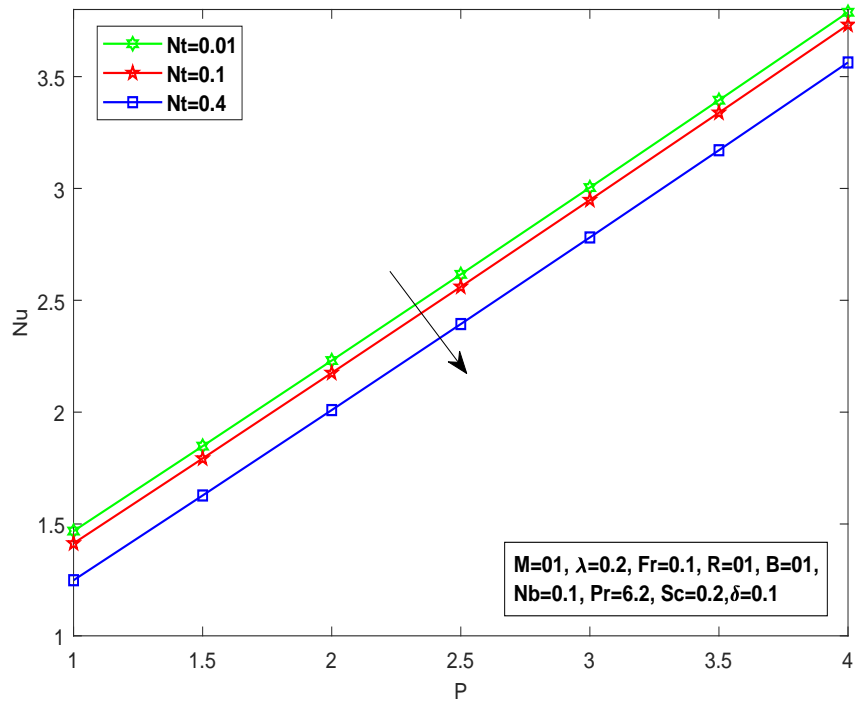


FIGURE 4.14: Nusselt number w.r.t P and N_t .

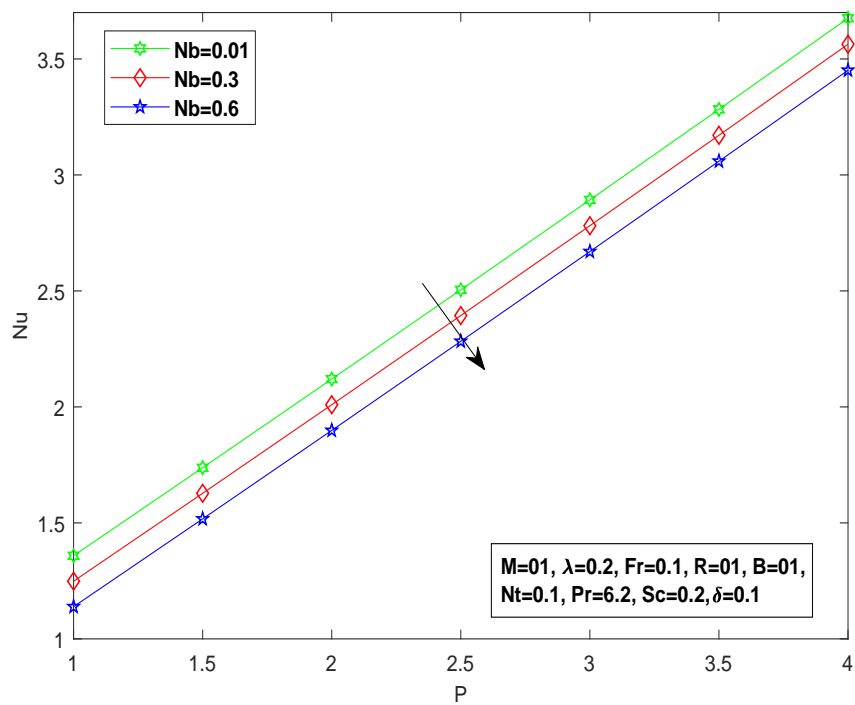


FIGURE 4.15: Nusselt number w.r.t P and N_b .

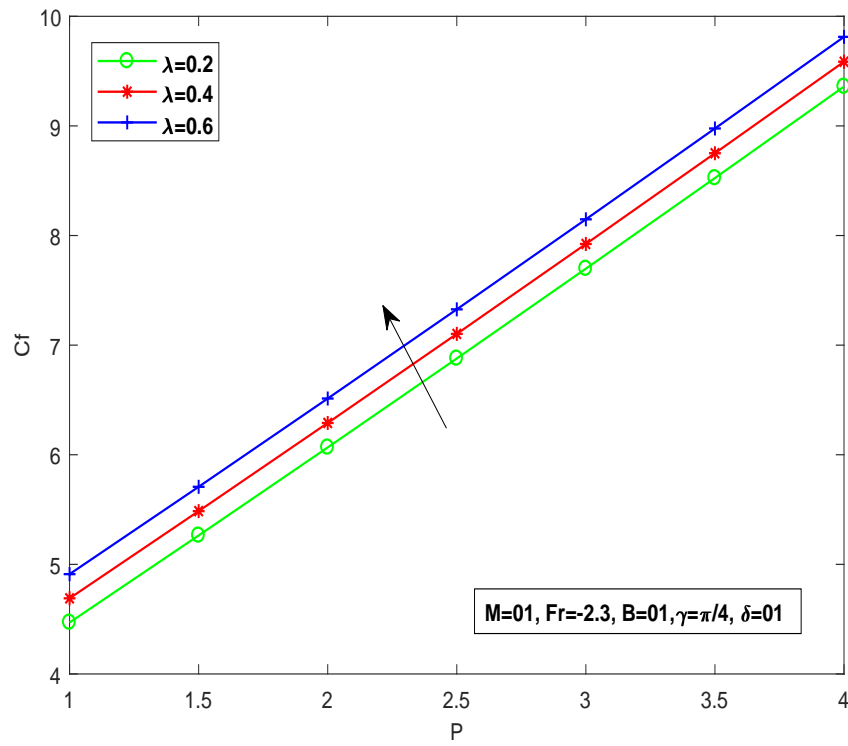


FIGURE 4.16: Variation in C_f for porosity factor λ .

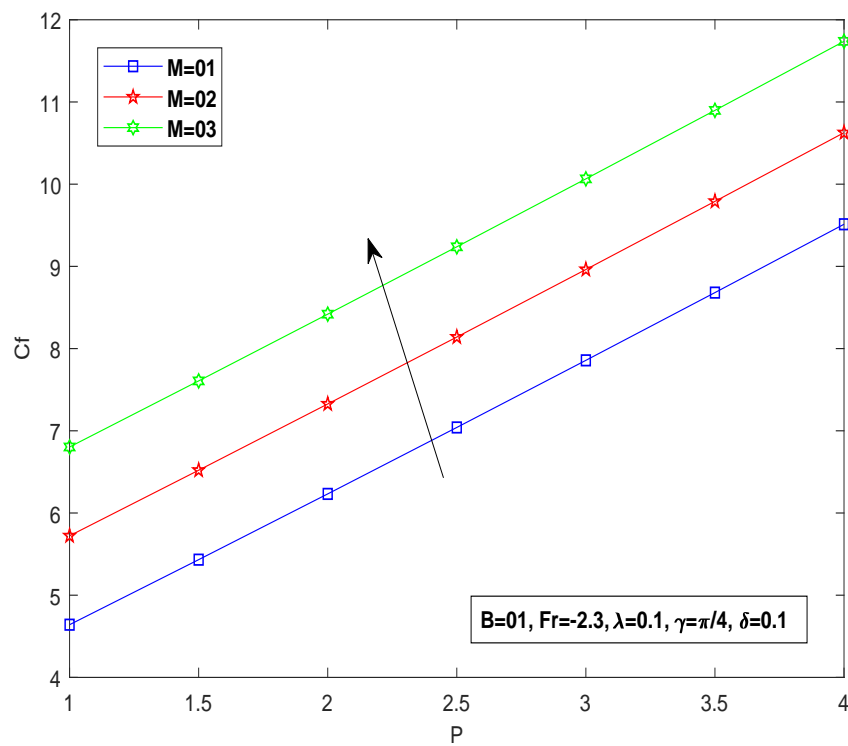


FIGURE 4.17: Variation in C_f for magnetic parameter M .

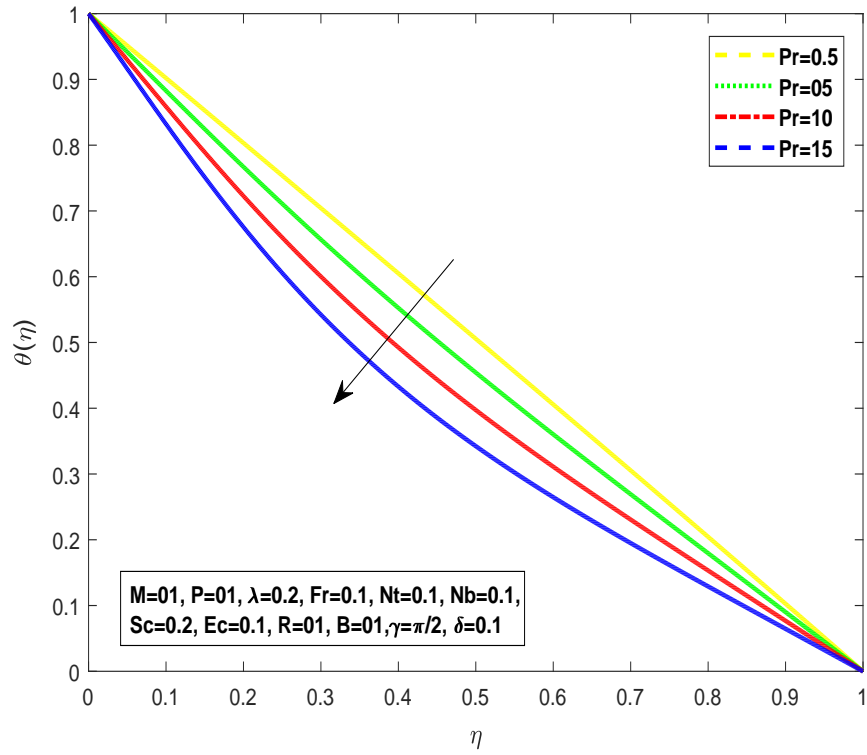


FIGURE 4.18: Consequences of Pr on $\theta(\eta)$.

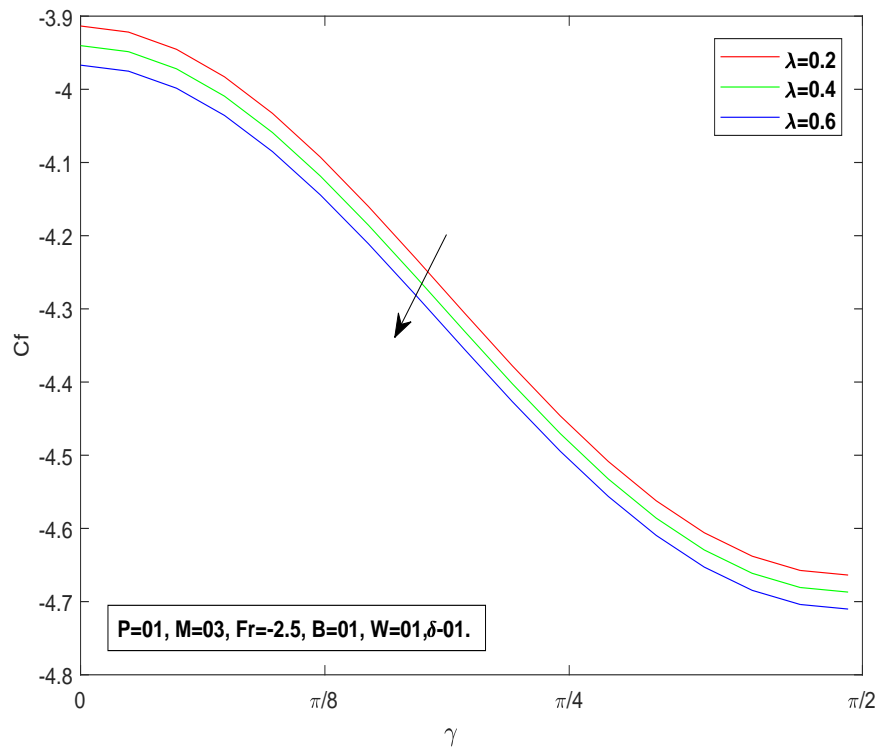


FIGURE 4.19: Skin friction w.r.t γ and λ .

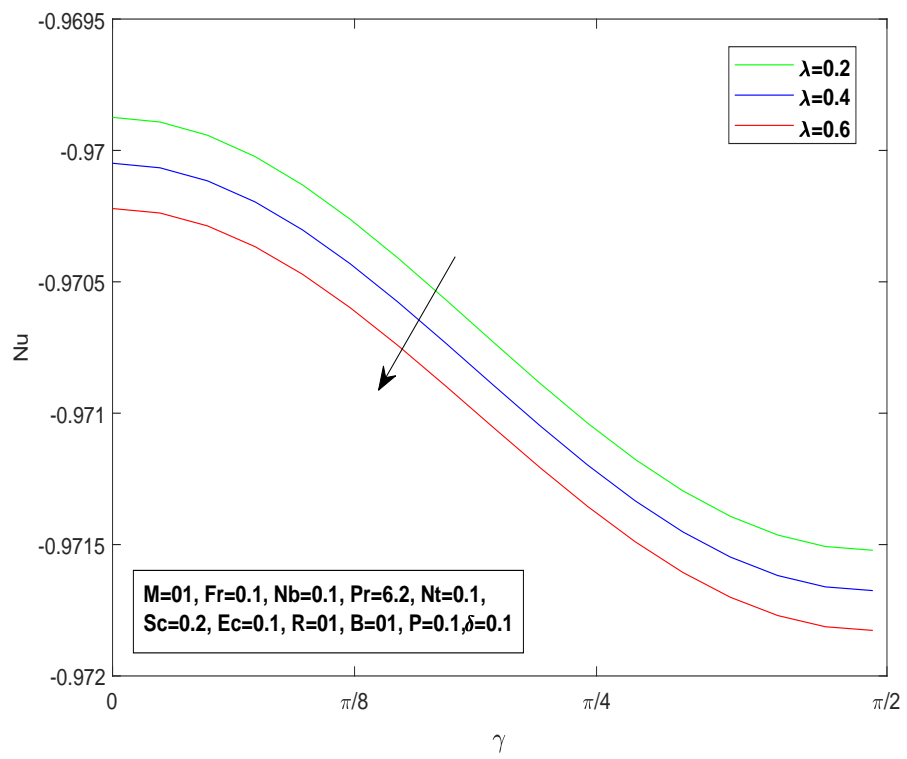


FIGURE 4.20: Nusselt number w.r.t γ and λ .

Chapter 5

Conclusion

In this thesis, the research work of Rasool et al.[1] is reviewed and extended with the effect of inclined magnetic field, Casson Fluid, viscous Dissipation, Brownian motion, thermophoresis diffusion and chemical reaction. First of all, momentum, energy and concentration equations are transformed into the ODEs via way of means of the similarity transformations. By the use of the shooting technique, numerical answer has been determined for the converted ODEs. Using unique values of the governing physical parameters, the consequences are provided with inside the form of graphs for velocity, temperature and concentration profiles. The achievements of the contemporary studies can be summarized as below:

- Velocity field suggests a decrease for large Forchheimer number. The drag force coefficient is liable for this trend.
- The effect of magnetic field is inversely associated with the fluid flow. A decline is observed in the velocity profile.
- For larger values of viscosity parameter, the inverse relation of kinematic viscosity confirms a decline in the velocity field.
- The non-predictive motion of nano particles, due to the Brownian diffusion rises for more potent thermophoretic force ensuring a speedy transport from warm region to the colder region.

-
- For larger values of viscosity parameter, an enhancement in the concentration distribution is observed.
 - The rate of heat flux reduces for Brownian diffusion and thermophoresis.
 - Skin-friction gets enhancement for accelerated porosity aspect and magnetic parameter.
 - For the increment of porosity factor (λ) and the angle of magnetic inclination (γ), the skin friction (C_f) decreases and the Nusselt number (Nu) decreases. Moreover, both skin friction and Nusselt number are decreasing function of angle of inclination.

Bibliography

- [1] G. Rasool, W. A. Khan, S. M. Bilal, and I. Khan, “Mhd squeezed darcy–forchheimer nanofluid flow between two h–distance apart horizontal plates,” *Open Physics*, vol. 18, no. 1, pp. 1100–1107, 2020.
- [2] M. M. Rashidi, H. Shahmohamadi, and S. Dinarvand, “Analytic approximate solutions for unsteady two-dimensional and axisymmetric squeezing flows between parallel plates,” *Mathematical problems in engineering*, vol. 2008, 2008.
- [3] T. Hayat, A. Qayyum, and A. Alsaedi, “Three-dimensional mixed convection squeezing flow,” *Applied Mathematics and Mechanics*, vol. 36, no. 1, pp. 47–60, 2015.
- [4] T. Hayat, A. Yousaf, M. Mustafa, and S. Obaidat, “Mhd squeezing flow of second-grade fluid between two parallel disks,” *International journal for numerical methods in fluids*, vol. 69, no. 2, pp. 399–410, 2012.
- [5] T. Hayat, T. Muhammad, A. Qayyum, A. Alsaedi, and M. Mustafa, “On squeezing flow of nanofluid in the presence of magnetic field effects,” *Journal of Molecular Liquids*, vol. 213, pp. 179–185, 2016.
- [6] H. Shahmohamadi and M. M. Rashidi, “Vim solution of squeezing mhd nanofluid flow in a rotating channel with lower stretching porous surface,” *Advanced Powder Technology*, vol. 27, no. 1, pp. 171–178, 2016.
- [7] A. Rostami, K. Hosseinzadeh, and D. Ganji, “Hydrothermal analysis of ethylene glycol nanofluid in a porous enclosure with complex snowflake shaped inner wall,” *Waves in Random and Complex Media*, vol. 32, no. 1, pp. 1–18, 2022.

-
- [8] Z. Shah, M. Sheikholeslami, P. Kumam, *et al.*, “Influence of nanoparticles inclusion into water on convective magneto hydrodynamic flow with heat transfer and entropy generation through permeable domain,” *Case Studies in Thermal Engineering*, vol. 21, p. 100732, 2020.
- [9] S. U. Choi and J. A. Eastman, “Enhancing thermal conductivity of fluids with nanoparticles,” tech. rep., Argonne National Lab.(ANL), Argonne, IL (United States), 1995.
- [10] S. Parvin and A. Chamkha, “An analysis on free convection flow, heat transfer and entropy generation in an odd-shaped cavity filled with nanofluid,” *International Communications in Heat and Mass Transfer*, vol. 54, pp. 8–17, 2014.
- [11] A. Zaraki, M. Ghalambaz, A. J. Chamkha, M. Ghalambaz, and D. De Rossi, “Theoretical analysis of natural convection boundary layer heat and mass transfer of nanofluids: effects of size, shape and type of nanoparticles, type of base fluid and working temperature,” *Advanced Powder Technology*, vol. 26, no. 3, pp. 935–946, 2015.
- [12] P. S. Reddy and A. J. Chamkha, “Soret and dufour effects on mhd convective flow of Al_2O_3 –water and TiO_2 –water nanofluids past a stretching sheet in porous media with heat generation/absorption,” *Advanced Powder Technology*, vol. 27, no. 4, pp. 1207–1218, 2016.
- [13] A. Chamkha, M. Ismael, A. Kasaeipoor, and T. Armaghani, “Entropy generation and natural convection of CuO -water nanofluid in c-shaped cavity under magnetic field,” *Entropy*, vol. 18, no. 2, p. 50, 2016.
- [14] G. Rasool, A. Shafiq, C. M. Khalique, and T. Zhang, “Magnetohydrodynamic darcy–forchheimer nanofluid flow over a nonlinear stretching sheet,” *Physica Scripta*, vol. 94, no. 10, p. 105221, 2019.
- [15] M. A. Ismael, T. Armaghani, and A. J. Chamkha, “Conjugate heat transfer and entropy generation in a cavity filled with a nanofluid-saturated porous

- media and heated by a triangular solid,” *Journal of the Taiwan Institute of Chemical Engineers*, vol. 59, pp. 138–151, 2016.
- [16] G. Rasool, T. Zhang, and A. Shafiq, “Second grade nanofluidic flow past a convectively heated vertical rigid plate,” *Physica Scripta*, vol. 94, no. 12, p. 125212, 2019.
- [17] L. Ali Lund, Z. Omar, I. Khan, J. Raza, M. Bakouri, and I. Tlili, “Stability analysis of darcy-forchheimer flow of casson type nanofluid over an exponential sheet: Investigation of critical points,” *Symmetry*, vol. 11, no. 3, p. 412, 2019.
- [18] G. Rasool and T. Zhang, “Darcy-forchheimer nanofluidic flow manifested with cattaneo-christov theory of heat and mass flux over non-linearly stretching surface,” *PLoS One*, vol. 14, no. 8, p. e0221302, 2019.
- [19] L. A. Lund, Z. Omar, I. Khan, and S. Dero, “Multiple solutions of Cu-NiO and Ag-CuO nanofluids flow over nonlinear shrinking surface,” *Journal of Central South University*, vol. 26, no. 5, pp. 1283–1293, 2019.
- [20] G. Rasool, A. Shafiq, and I. Tlili, “Marangoni convective nanofluid flow over an electromagnetic actuator in the presence of first-order chemical reaction,” *Heat Transfer Asian Research*, vol. 49, no. 1, pp. 274–288, 2020.
- [21] G. Rasool, A. Shafiq, and H. Durur, “Darcy-forchheimer relation in magneto-hydrodynamic jeffrey nanofluid flow over stretching surface,” *Discrete & Continuous Dynamical Systems-S*, vol. 14, no. 7, p. 2497, 2021.
- [22] A. P. Abraham, “Jd and mohanraj, m., thermodynamic performance of automobile air conditioners working with r430a as a drop-in substitute to r134a,” *Journal of Thermal Analysis and Calorimetry*, vol. 136, no. 5, pp. 2071–2086, 2018.
- [23] M. Sohail, R. Naz, and S. I. Abdelsalam, “On the onset of entropy generation for a nanofluid with thermal radiation and gyrotactic microorganisms through 3d flows,” *Physica Scripta*, vol. 95, no. 4, p. 045206, 2020.

- [24] M. Sohail and R. Naz, “Modified heat and mass transmission models in the magnetohydrodynamic flow of sutterby nanofluid in stretching cylinder,” *Physica A: Statistical Mechanics and its Applications*, vol. 549, p. 124088, 2020.
- [25] G. Rasool, T. Zhang, A. J. Chamkha, A. Shafiq, I. Tlili, and G. Shahzadi, “Entropy generation and consequences of binary chemical reaction on mhd darcy–forchheimer williamson nanofluid flow over non-linearly stretching surface,” *Entropy*, vol. 22, no. 1, p. 18, 2019.
- [26] I. Tlili and T. Alkanhal, “Nanotechnology for water purification: electrospun nanofibrous membrane in water and wastewater treatment. j water reuse desalination. 2019,” 2019.
- [27] I. Tlili, W. Khan, and K. Ramadan, “Mhd flow of nanofluid flow across horizontal circular cylinder: steady forced convection,” *Journal of Nanofluids*, vol. 8, no. 1, pp. 179–186, 2019.
- [28] A. Wakif, Z. Boulahia, A. Amine, I. Animasaun, M. Afridi, M. Qasim, and R. Sehaqui, “Magneto-convection of alumina-water nanofluid within thin horizontal layers using the revised generalized buongiorno’s model,” *Frontiers in Heat and Mass Transfer (FHMT)*, vol. 12, 2018.
- [29] A. Wakif, Z. Boulahia, and R. Sehaqui, “A semi-analytical analysis of electrothermo-hydrodynamic stability in dielectric nanofluids using buongiorno’s mathematical model together with more realistic boundary conditions,” *Results in Physics*, vol. 9, pp. 1438–1454, 2018.
- [30] A. Shafiq, G. Rasool, and C. M. Khalique, “Significance of thermal slip and convective boundary conditions in three dimensional rotating darcy–forchheimer nanofluid flow,” *Symmetry*, vol. 12, no. 5, p. 741, 2020.
- [31] K. Hosseinzadeh, S. Roghani, A. Mogharrebi, A. Asadi, M. Waqas, and D. Ganji, “Investigation of cross-fluid flow containing motile gyrotactic microorganisms and nanoparticles over a three-dimensional cylinder,” *Alexandria Engineering Journal*, vol. 59, no. 5, pp. 3297–3307, 2020.

- [32] K. Hosseinzadeh, A. Mogharrebi, A. Asadi, M. Sheikhshahrokhdehordi, S. Mousavisani, and D. Ganji, “Entropy generation analysis of mixture nanofluid (h₂o/c₂h₆o₂)–fe₃o₄ flow between two stretching rotating disks under the effect of mhd and nonlinear thermal radiation,” *International Journal of Ambient Energy*, vol. 43, no. 1, pp. 1045–1057, 2022.
- [33] Z. Shah, M. R. Hajizadeh, N. A. Alreshidi, W. Deebani, M. Shutaywi, *et al.*, “Entropy optimization and heat transfer modeling for lorentz forces effect on solidification of nepcm,” *International Communications in Heat and Mass Transfer*, vol. 117, p. 104715, 2020.
- [34] M. Sohail, Z. Shah, A. Tassaddiq, P. Kumam, and P. Roy, “Entropy generation in mhd casson fluid flow with variable heat conductance and thermal conductivity over non-linear bi-directional stretching surface,” *Scientific Reports*, vol. 10, no. 1, pp. 1–16, 2020.
- [35] W. Deebani, A. Tassaddiq, Z. Shah, A. Dawar, and F. Ali, “Hall effect on radiative casson fluid flow with chemical reaction on a rotating cone through entropy optimization,” *Entropy*, vol. 22, no. 4, p. 480, 2020.
- [36] Z. Shah, P. Kumam, A. Dawar, E. O. Alzahrani, and P. Thounthong, “Study of the couple stress convective micropolar fluid flow in a hall mhd generator system,” *Frontiers in Physics*, vol. 7, p. 171, 2019.
- [37] P. Forchheimer, “Wasserbewegung durch boden,” *Z. Ver. Deutsch, Ing.*, vol. 45, pp. 1782–1788, 1901.
- [38] M. Muskat and R. Wyckoff, “The flow of homogeneous fluids through porous media: Ann arbor,” *Michigan, JW Edwards*, 1946.
- [39] M. Seddeek, “Influence of viscous dissipation and thermophoresis on darcy–forchheimer mixed convection in a fluid saturated porous media,” *Journal of Colloid and interface Science*, vol. 293, no. 1, pp. 137–142, 2006.
- [40] T. Hayat, M. I. Khan, T. A. Khan, M. I. Khan, S. Ahmad, and A. Alsaedi, “Entropy generation in darcy-forchheimer bidirectional flow of water-based

- carbon nanotubes with convective boundary conditions,” *Journal of Molecular Liquids*, vol. 265, pp. 629–638, 2018.
- [41] M. A. Sadiq and T. Hayat, “Darcy–forchheimer flow of magneto maxwell liquid bounded by convectively heated sheet,” *Results in Physics*, vol. 6, pp. 884–890, 2016.
- [42] J. C. Umavathi, O. Ojjela, and K. Vajravelu, “Numerical analysis of natural convective flow and heat transfer of nanofluids in a vertical rectangular duct using darcy-forchheimer-brinkman model,” *International Journal of Thermal Sciences*, vol. 111, pp. 511–524, 2017.
- [43] T. Hayat, F. Shah, M. I. Khan, and A. Alsaedi, “Framing the performance of heat absorption/generation and thermal radiation in chemically reactive darcy-forchheimer flow,” *Results in Physics*, vol. 7, pp. 3390–3395, 2017.
- [44] R. W. Fox, A. McDonald, and P. Pitchard, *Introduction to Fluid Mechanics*. 2006.
- [45] R. Bansal, *A Textbook of Fluid Mechanics and Dydraulic Machines*. Laxmi publications, 2004.
- [46] J. N. Reddy and D. K. Gartling, *The Finite Element Method in Heat Transfer and Fluid Dynamics*. CRC press, 2010.
- [47] P. A. Davidson and A. Thess, *Magnetohydrodynamics*, vol. 418. Springer Science & Business Media, 2002.
- [48] R. W. Fox, A. T. McDonald, and P. J. Pritchard, “Introduction to fluid mechanics, john wiley&sons,” *Inc., New York*, 1994.
- [49] Y. Cengel and J. Cimbala, *EBOOK: Fluid Mechanics Fundamentals and Applications (SI units)*. McGraw Hill, 2013.
- [50] J. Kunes, *Dimensionless physical quantities in science and engineering*. Elsevier, 2012.

- [51] B. Lindner, “The diffusion coefficient of nonlinear brownian motion,” *New Journal of Physics*, vol. 9, no. 5, p. 136, 2007.
- [52] D. Braun and A. Libchaber, “Trapping of dna by thermophoretic depletion and convection,” *Physical review letters*, vol. 89, no. 18, p. 188103, 2002.